

MATERIALS CHARACTERISATION AT MULTIPLE LENGTHSCALES VIA COHERENT DIFFRACTION AND NEUTRON BRAGG DIFFRACTION

A/Prof Brian Abbey
Department of Chemistry and Physics,
La Trobe University

Motivation

N. A. FLECK, G. M. MULLER, M. F. ASHBY and J. W. HUTCHINSON
Acta metall, mater. Vol. 42, No. 2, pp. 475-487, 1994 [1]

“Several observed plasticity phenomena display a size effect whereby the **smaller** is the size the **stronger** is the response... The effect becomes pronounced when the indent size, grain size or particle spacing lies **below approximately $10\ \mu\text{m}$** .”



Motivation

N. A. FLECK, G. M. MULLER, M. F. ASHBY and J. W. HUTCHINSON
Acta metall, mater. Vol. 42, No. 2, pp. 475-487, 1994 [1]

“Several observed plasticity phenomena display a size effect whereby the **smaller** is the size the **stronger** is the response... The effect becomes pronounced when the indent size, grain size or particle spacing lies **below approximately $10\ \mu\text{m}$** .”

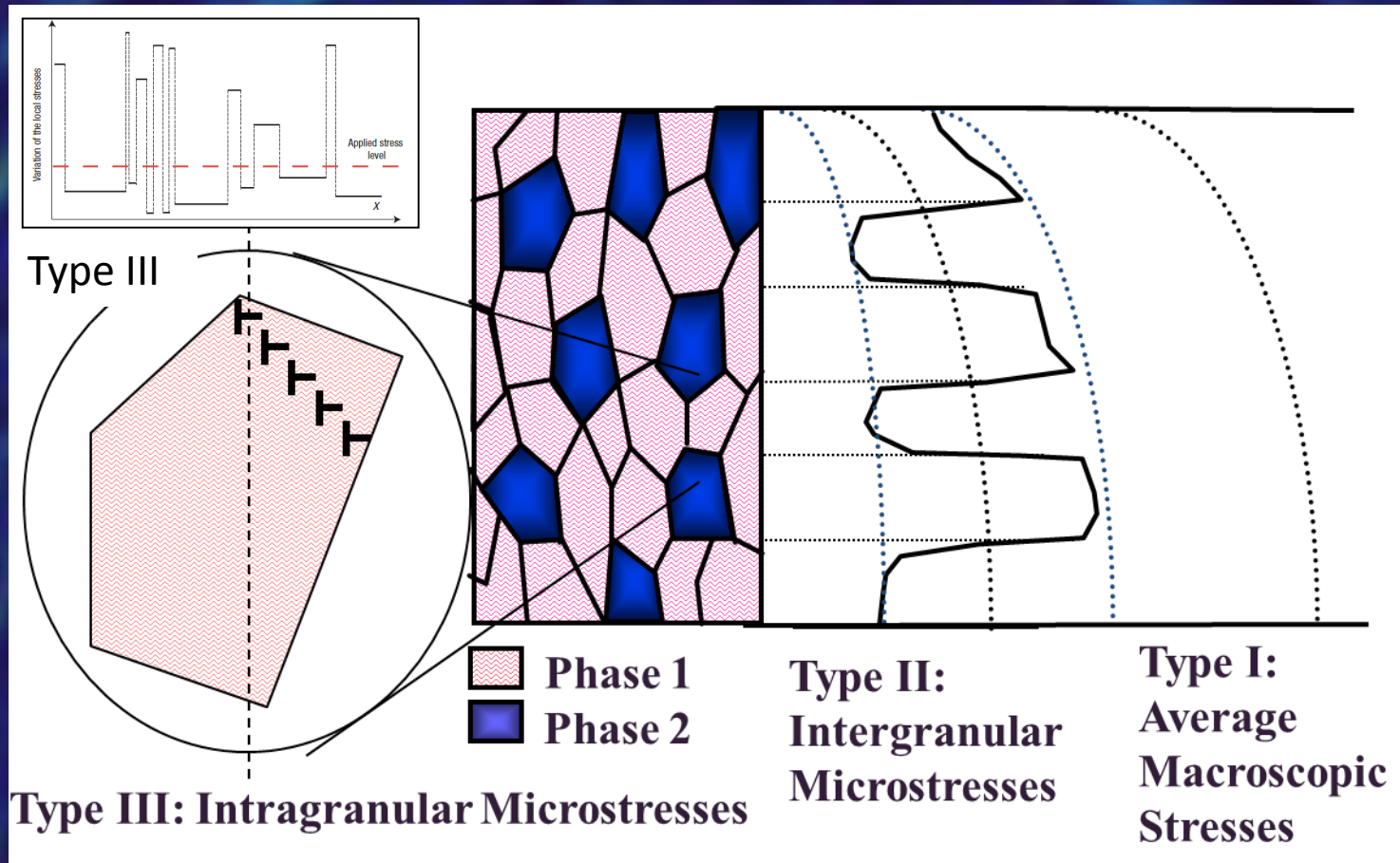
There is a gap in our current understanding and prediction of defect behaviour at these key length scales that is driving the development of new techniques.



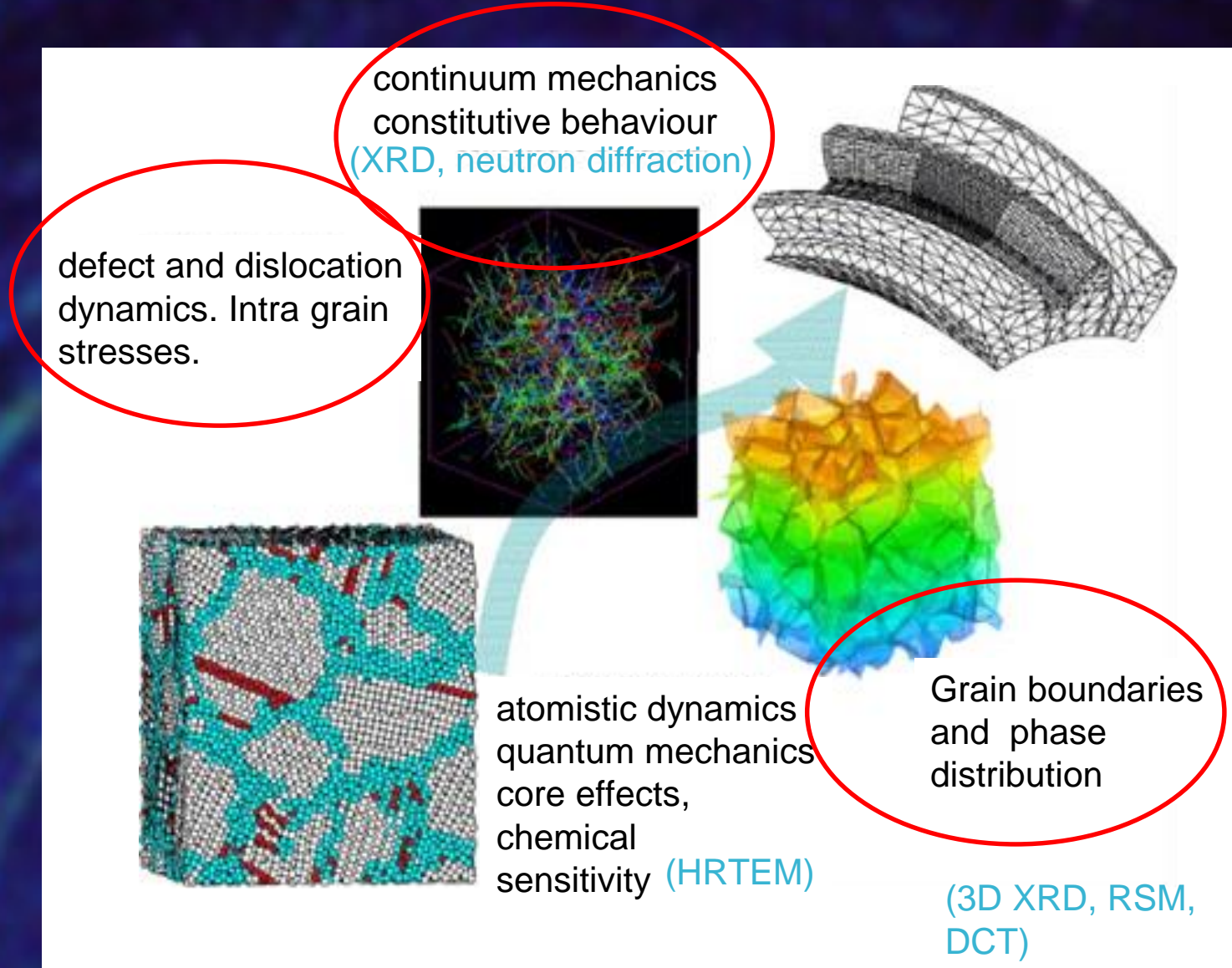
Type I: Stress varying on engineering scales (\sim mm),
macrostress

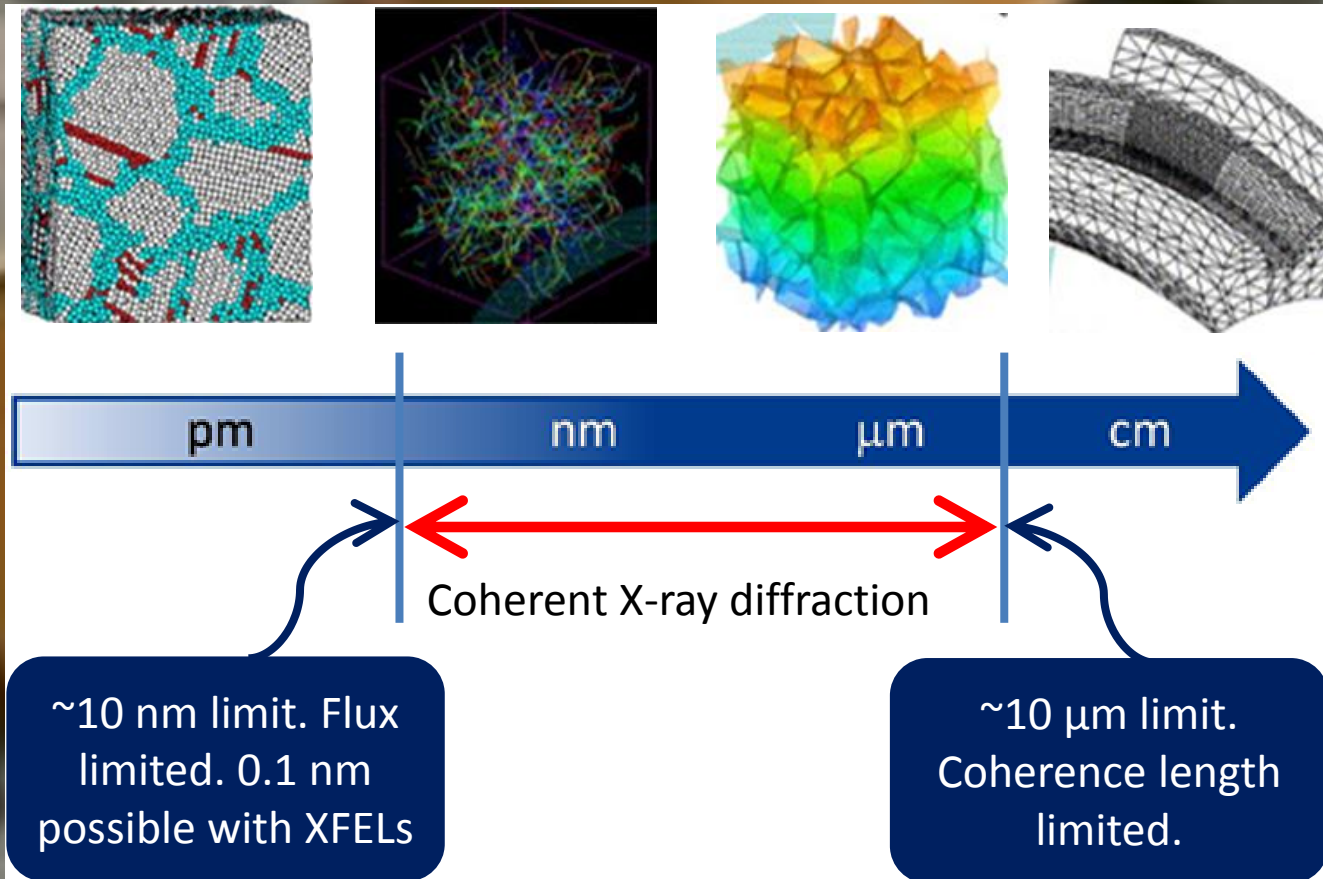
Type II: Stress varying on grain size scales (\sim μ m), e.g.
interphase

Type III: Stress due to lattice defects (\sim nm), e.g. dislocations



Predictive models

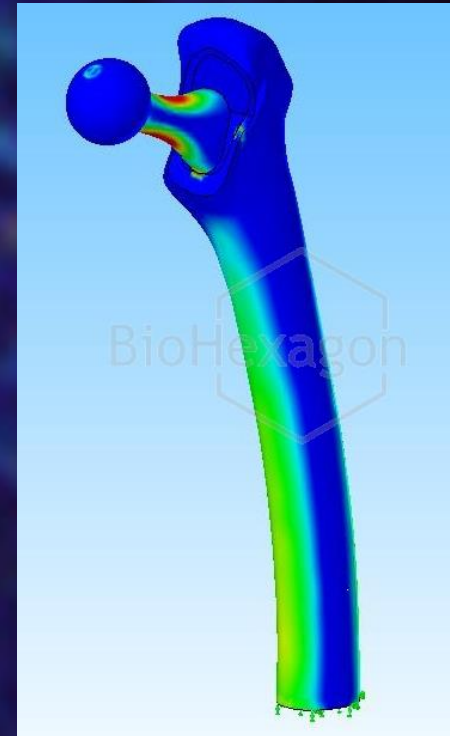






TOMOGRAPHIC IMAGING OF ELASTIC STRAIN

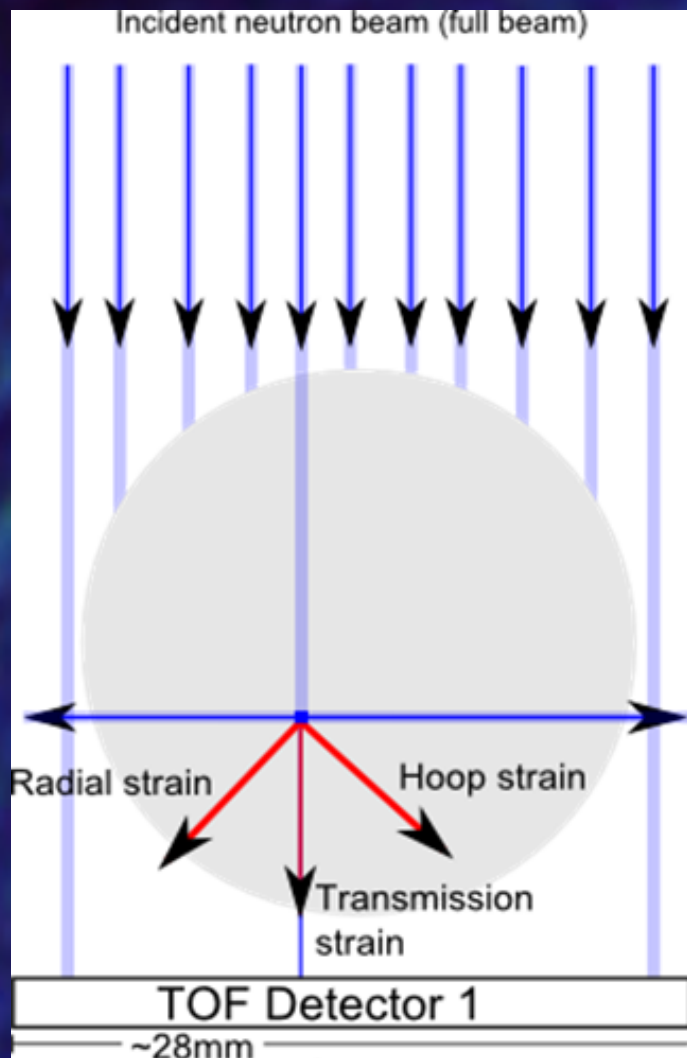
- Knowledge of residual elastic strain profile key to predicting deformation and fatigue lifetimes of engineering components
- Current techniques for non-destructive strain measurements use scanning.
- Neutron Bragg-edge transmission measurements provide information on the average strain throughout the whole sample.



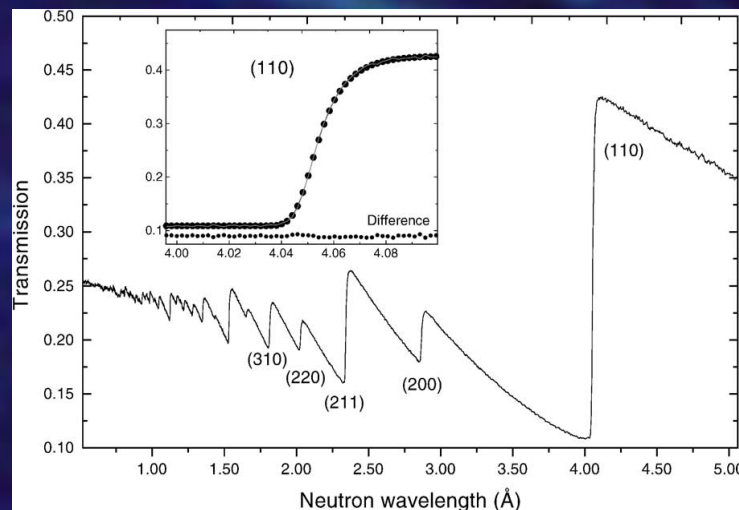


H. Kirkwood,
2nd year PhD

TOMOGRAPHIC IMAGING OF ELASTIC STRAIN



Typical energy resolved
spectrum

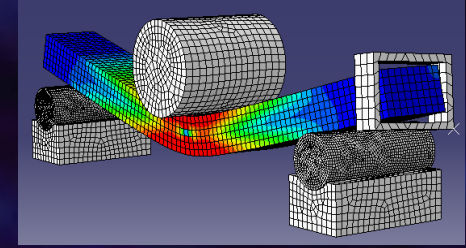


$$\varepsilon = \frac{d - d_0}{d_0} = \frac{t - t_0}{t_0}$$

Detector:
Microchannel Plate with TimePix readout
512 x 512 pixels of 55 x 55 μm ,
1 μs temporal resolution

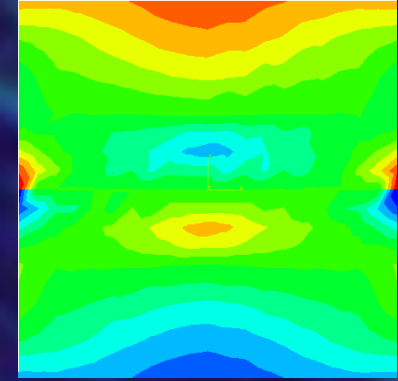
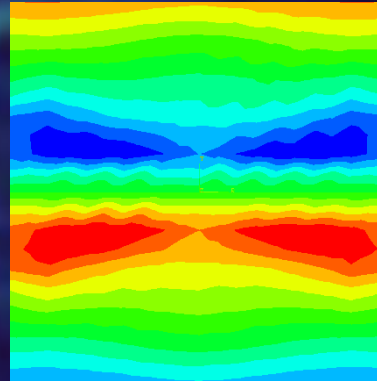


H. Kirkwood, 'Bent Beam' example:
2nd year PhD



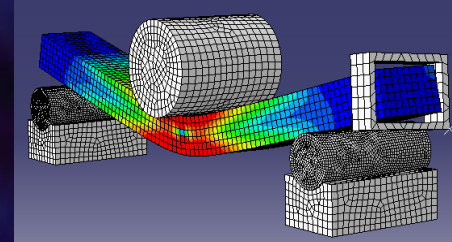
Radial

Hoop



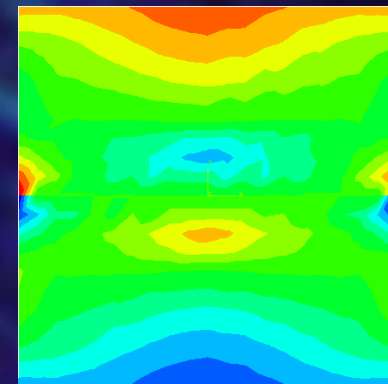
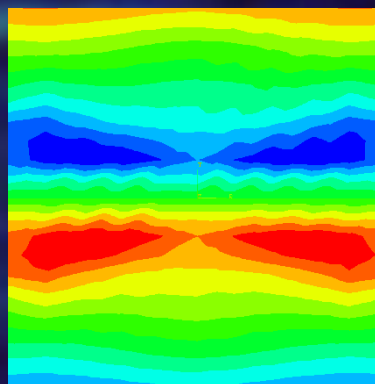


H. Kirkwood, 'Bent Beam' example:
2nd year PhD



Radial

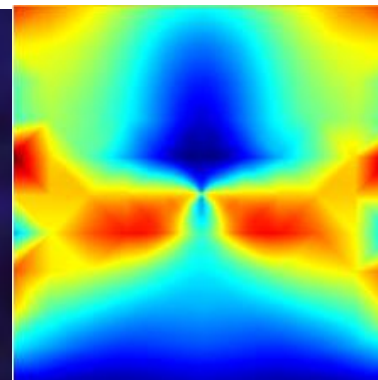
Hoop



$$\epsilon_y = \epsilon_{rr} \sin^2 \theta + \epsilon_{\theta\theta} \cos^2 \theta$$

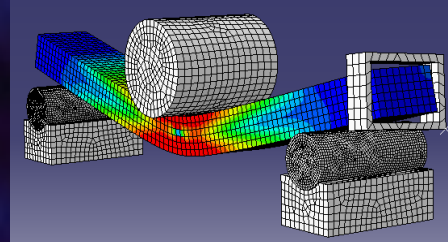
Transmitted (0 deg)

y ↑



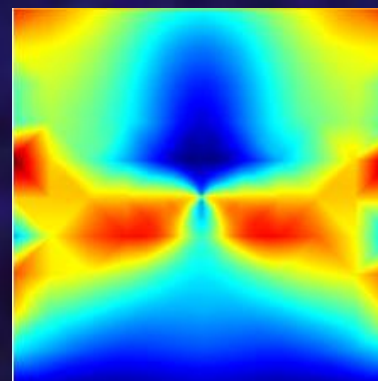
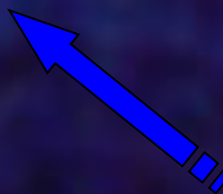
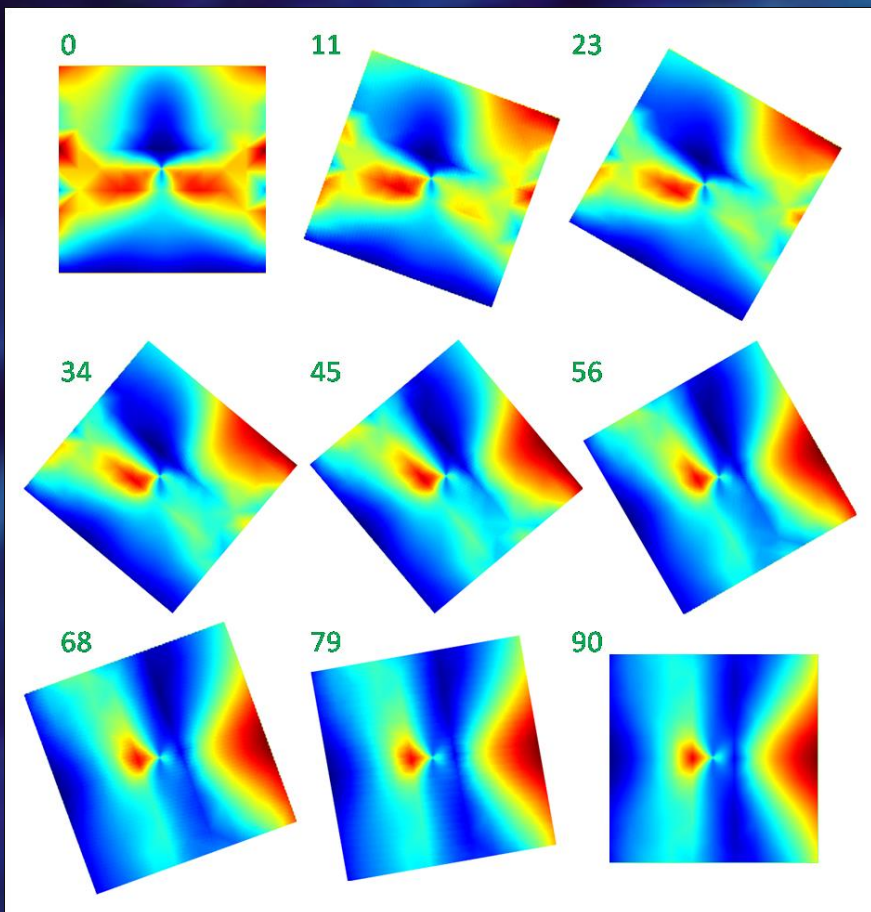
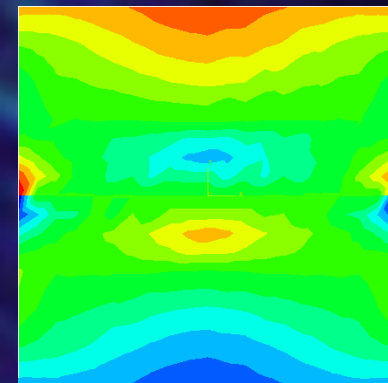
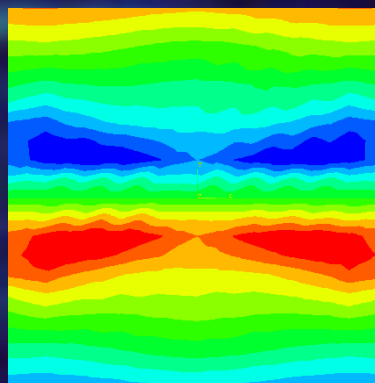


H. Kirkwood, 'Bent Beam' example: 2nd year PhD



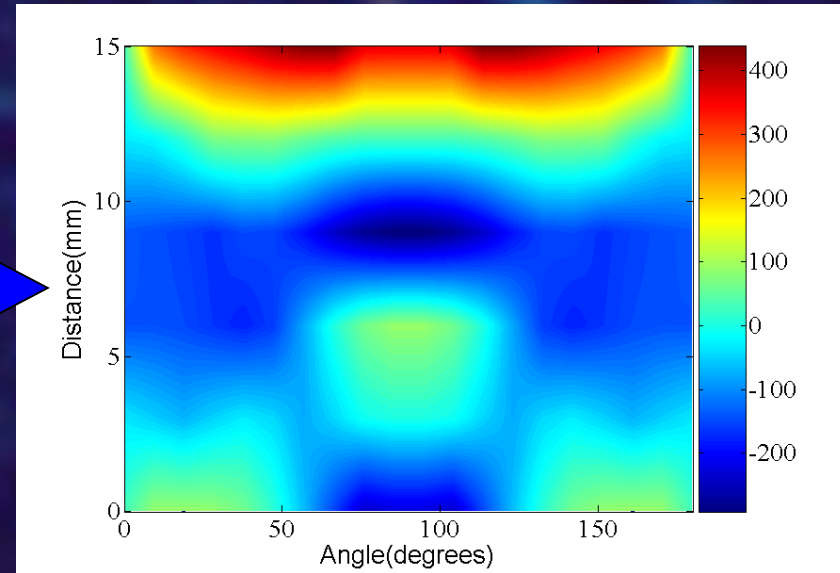
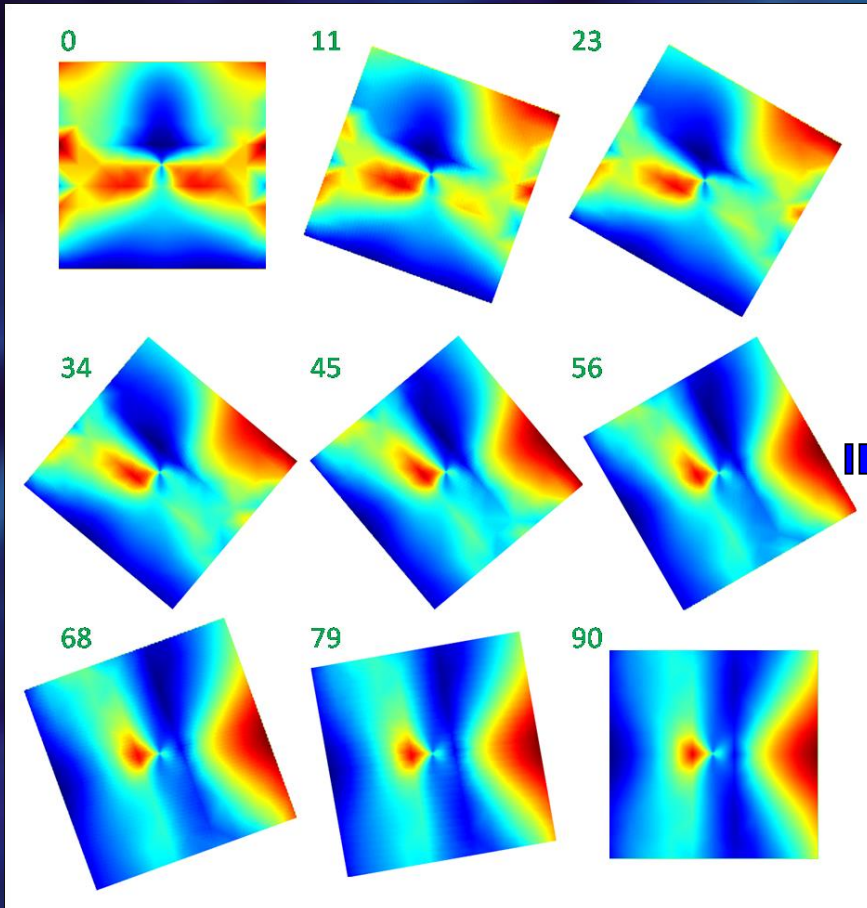
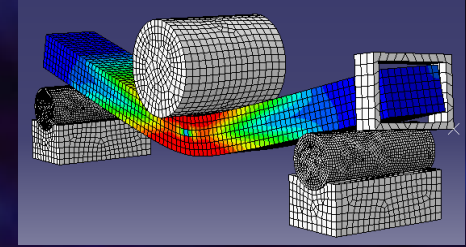
Radial

Hoop





H. Kirkwood, 'Bent Beam' example: 2nd year PhD



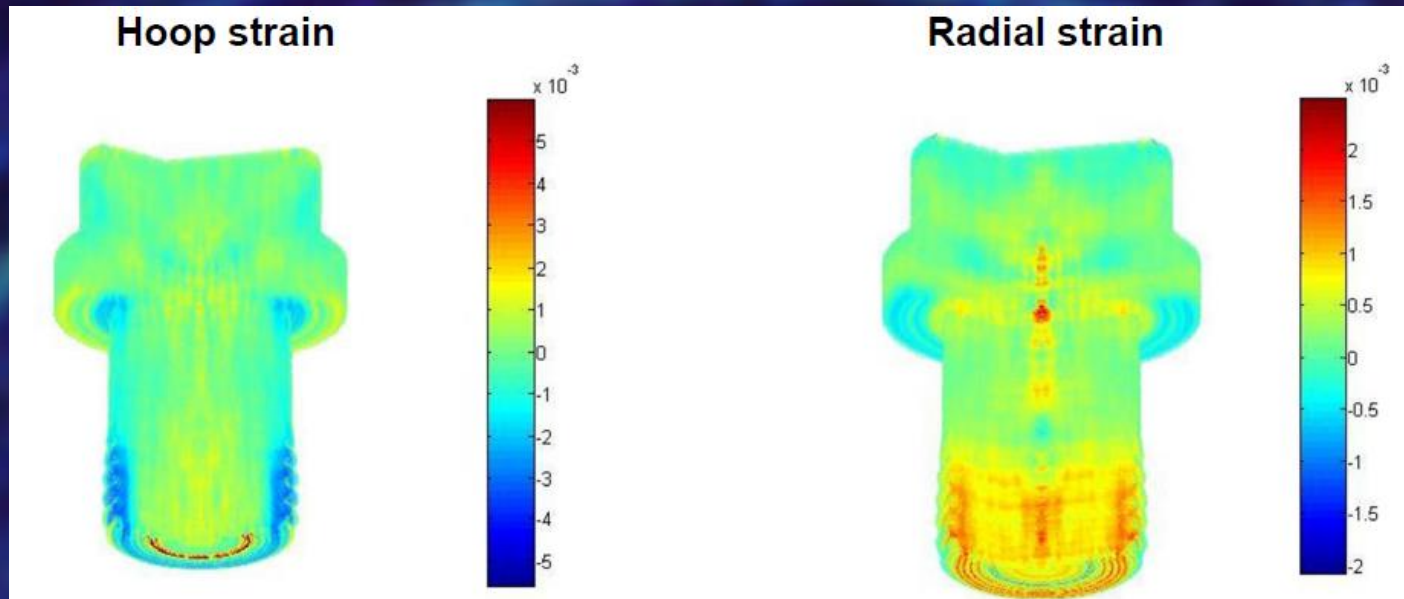
$$\varepsilon_{rr} = \frac{\partial u_r}{\partial r} = \frac{\partial}{\partial r} (r\varepsilon_{\theta\theta})$$



H. Kirkwood,
2nd year PhD

TOMOGRAPHIC IMAGING OF ELASTIC STRAIN

$$\mathcal{R}\{E_T(r, \theta)\}(t, \phi) = T_1 \times p_{\phi_1=0}(t) \times \frac{\varepsilon_{\theta\theta}(R_1) \cos^2(\phi) + \varepsilon_{rr}(R_1) \sin^2(\phi)}{\varepsilon_{\theta\theta}(R_1)}$$



Abbey, B., Zhang, S. Y., Vorster, W. J. J., et al. *Proc. Engineering* **1**(1), 185–188, (2009).

Abbey, B., Zhang, S. Y., Vorster, W. J., et al. *NIMB*, **270**, 28–35 January (2012).

Abbey, B., Zhang, S. Y., Xie, M., et al. *IMJR*, **103**, 234–241 (2012).

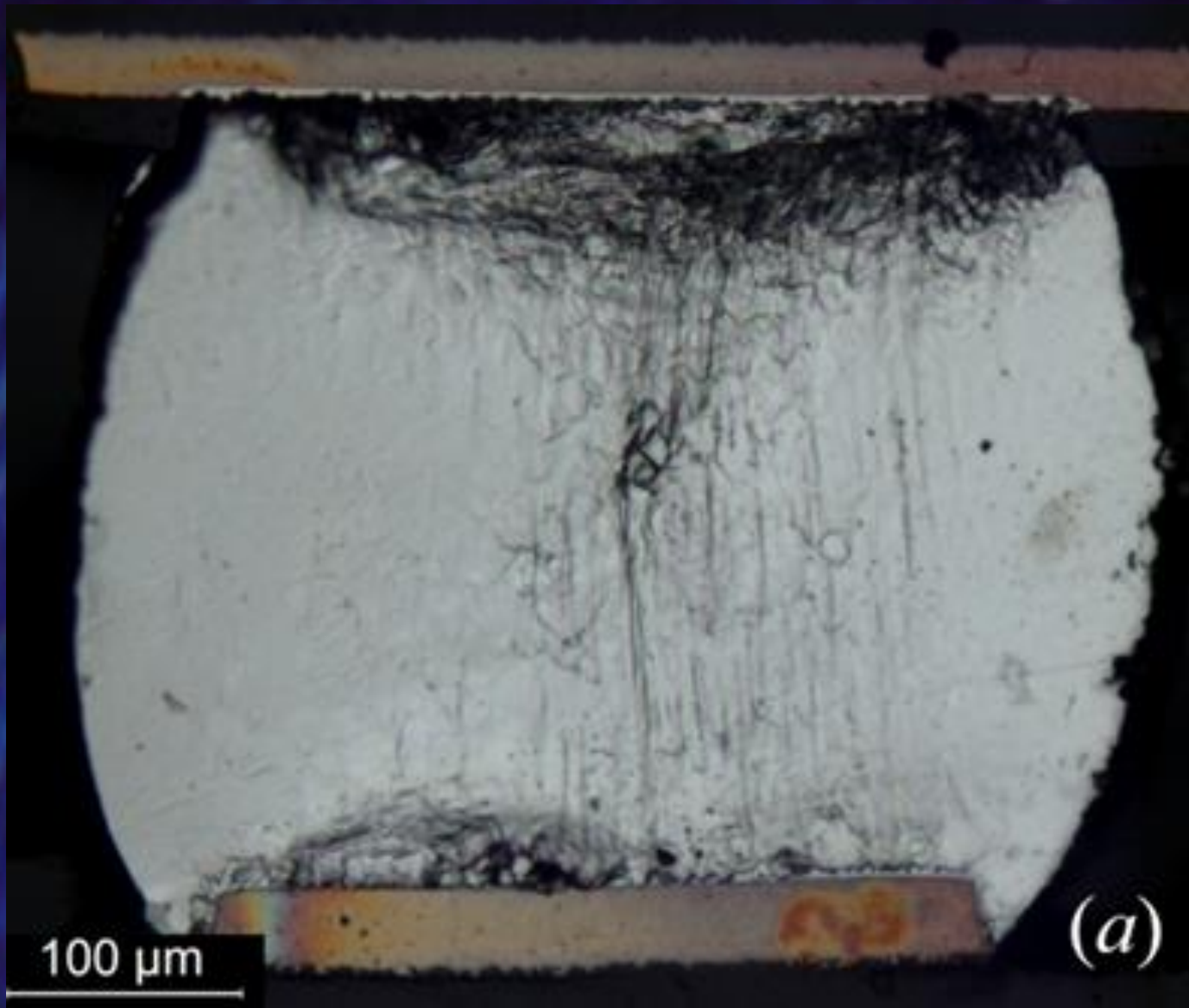
Kirkwood, H. J., Abbey, B.* , Quiney, H. M., et al. In *ACA Trans.*, (2013).

Kirkwood, H. J., Zhang, S. Y., Tremsin, A. S., Lie, W. Korsunsky, A. M., Baimpas, N.

Abbey, B* , *Materials Today*, (2014) (Accepted)

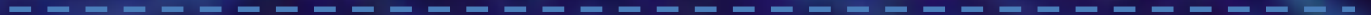
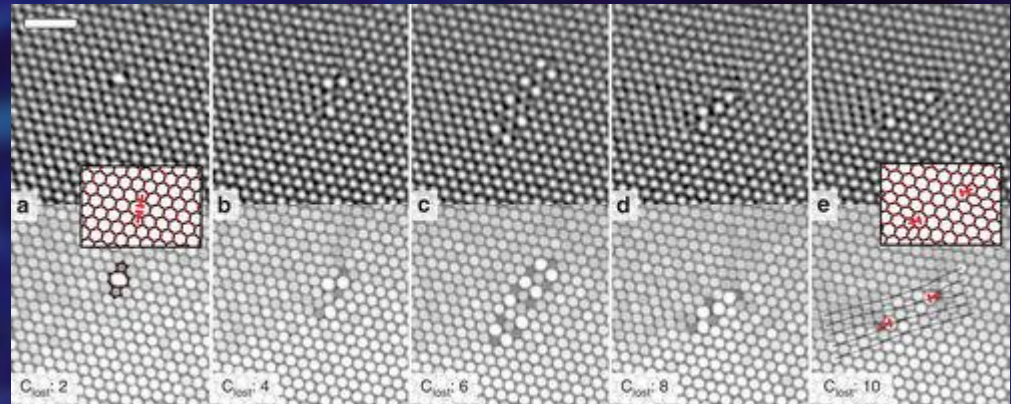
patent: B.Abbey, "System and Method for Three-Dimensional Strain Mapping", March 2014

WHAT ABOUT PLASTIC STRAIN?



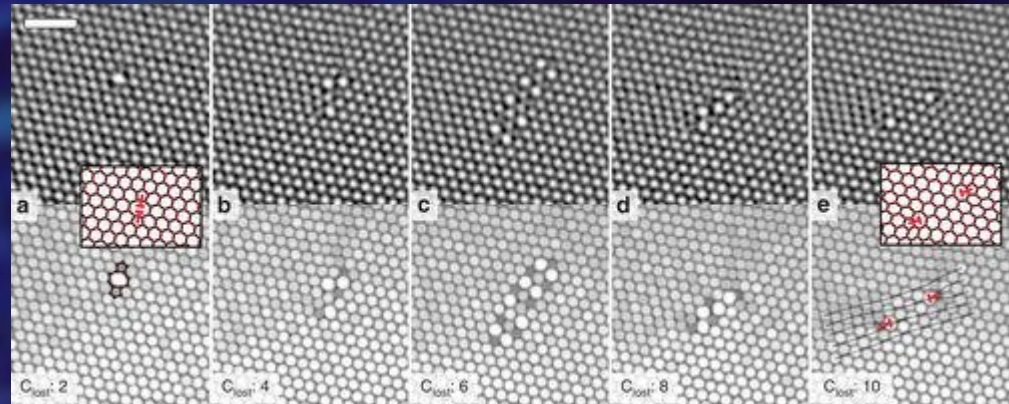
How can X-rays image dislocations?

HRTEM image
of the creation
of two edge
dislocations [2]



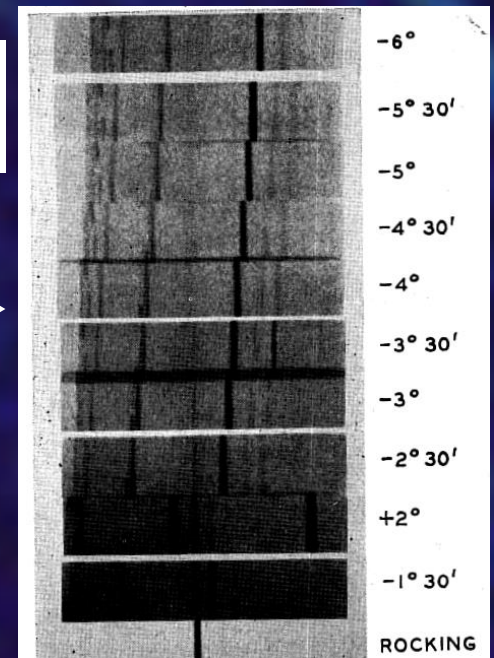
How can X-rays image dislocations?

HRTEM image
of the creation
of two edge
dislocations [2]



X-Ray Studies of Surface Layers of Crystals
By **ELIZABETH J. ARMSTRONG** [3]

Rocking curve photographs
of “disturbed quartz”



Bell System Technical Journal
Volume 25, Issue 1, pages 136–155, January
1946

How can X-rays image dislocations?

Direct Observation of Individual Dislocations by X-Ray Diffraction [4]

A. R. LANG

*Division of Engineering and Applied Physics, Harvard University,
Cambridge 38, Massachusetts
(Received October 21, 1957)*

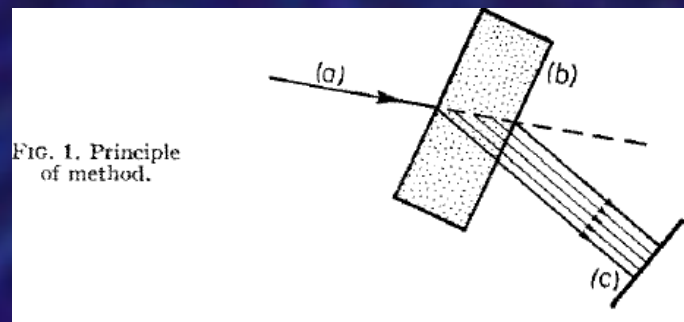
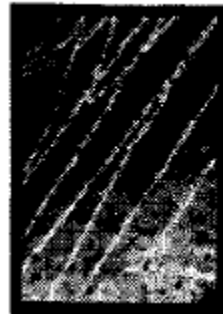
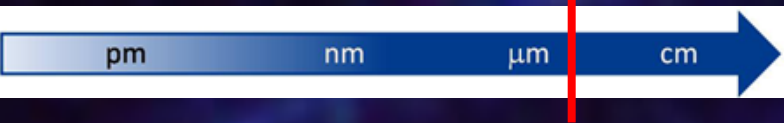


FIG. 3. Infrared transmission micrograph.



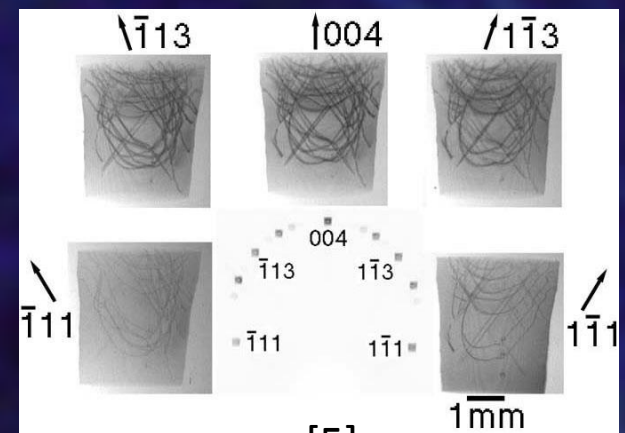
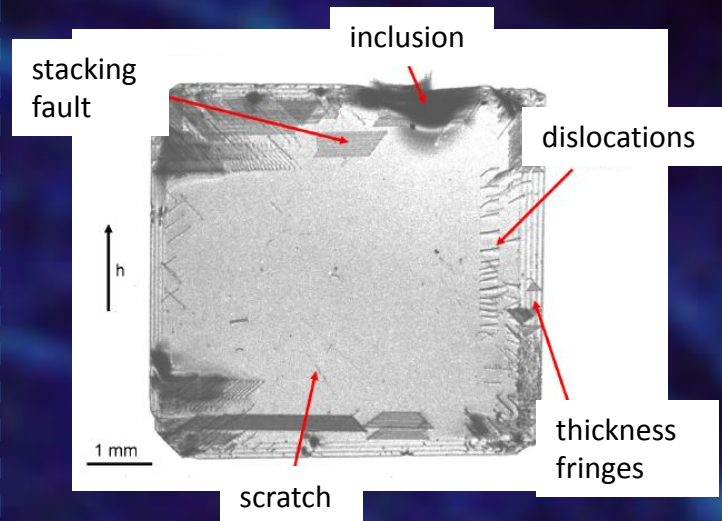
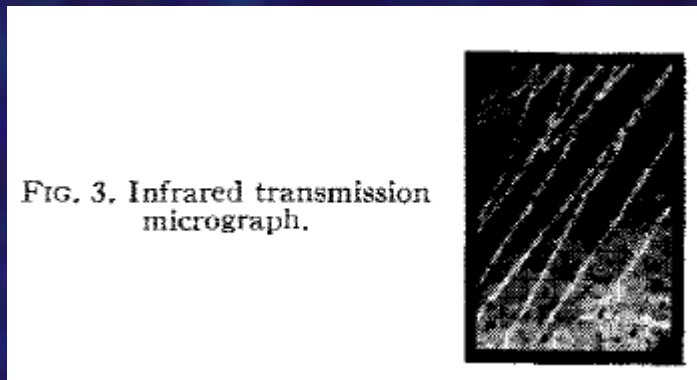
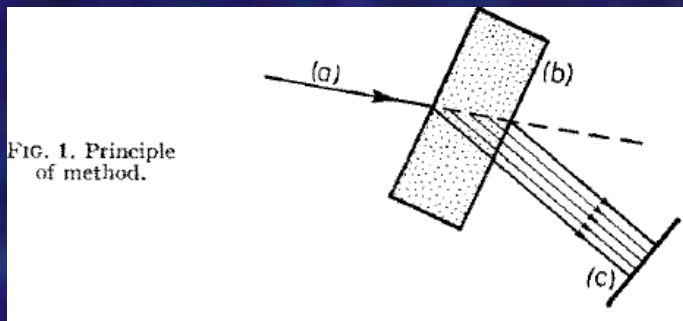


How can X-rays image dislocations?

Direct Observation of Individual Dislocations by X-Ray Diffraction [4]

A. R. LANG

*Division of Engineering and Applied Physics, Harvard University,
Cambridge 38, Massachusetts
(Received October 21, 1957)*



What happens in polycrystals?

Nickel Foil < 2% plastic strain. Energy scan over 2000 eV carried out at the XFM beamline, Australian Synchrotron (2014).



- Diffraction from sub-grain regions.
- Most information lost at a single energy.
- No direct correspondence between real and reciprocal space information.

XRT: SUMMARY



X-ray Topography (XRT) is a very mature technique (in development since the 1930's!).

Great technique for brittle materials where crystallinity is good, not so great for ductile.

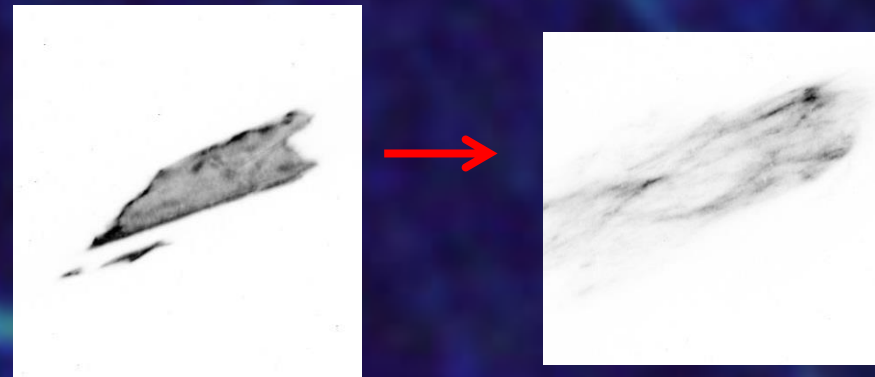
3D dislocation imaging demonstrated by Ludwig in 2001, 5 years before Banard achieved the same feat with electrons.

Can image dislocation dynamics in real-time (current max temporal resolution ~ 10 Hz).

However...

Spatial resolution is limited to $\sim 5 \mu\text{m}$, low levels of plastic strain required.

For plastically deformed materials need to consider sub-grain structure...

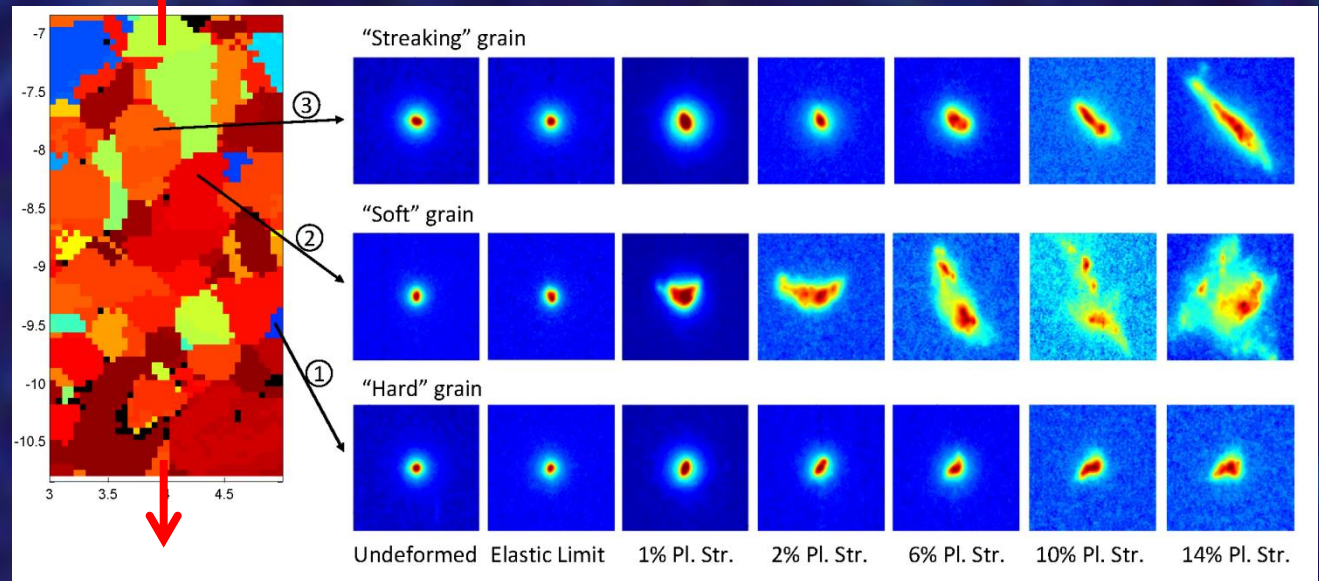
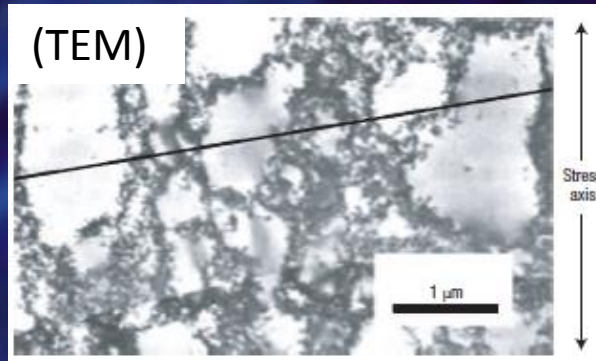
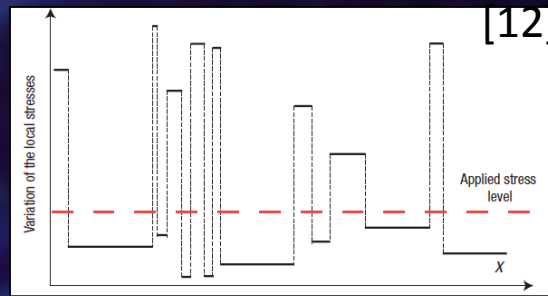


Sub-grain deformation

What happens inside the grain?

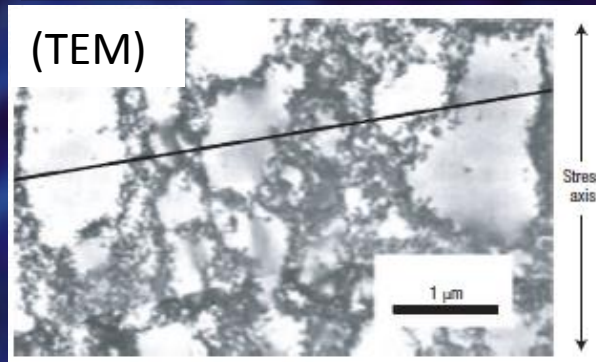
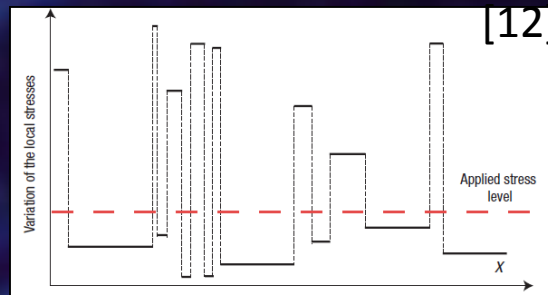
Formation of **CELL** and **WALL** structures. (Mughrabi et al.)

Lattice rotation and mosaicing



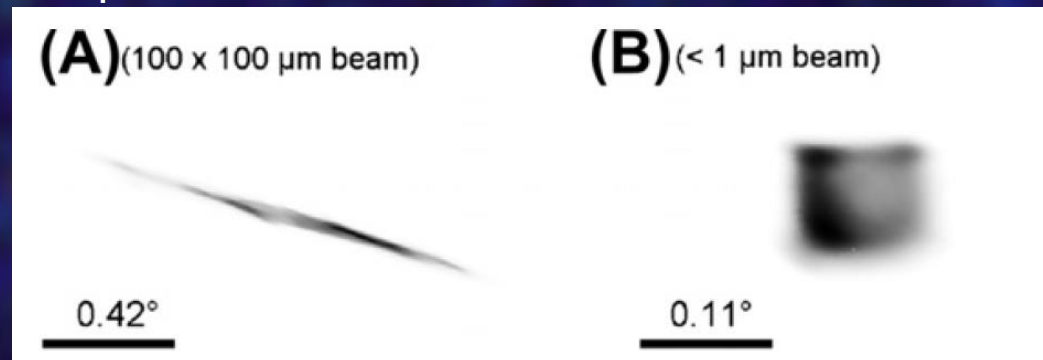
Sub-grain deformation

What happens inside the grain?



Deconvolution of real and reciprocal space information is most easily achieved using a small incident beam.

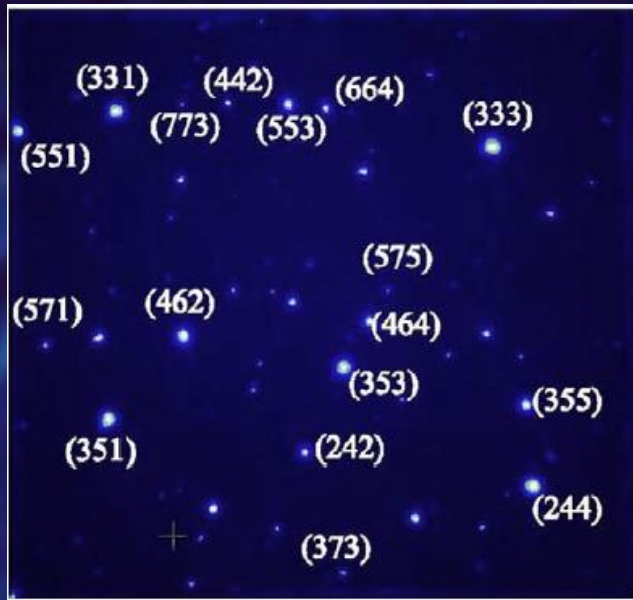
4% plastic strain:



Full grain topograph 0.1 x 0.1 mm beam - 1 position (2 mins)

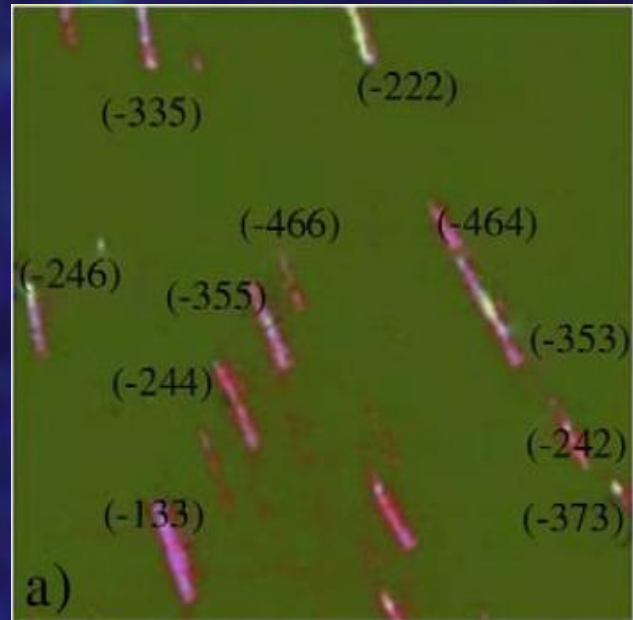


MICROBEAM LAUE



Elastic strain example (stainless steel).

- Need to know unstrained lattice parameter (i.e. needs to be of known composition).
- Determine elastic strain tensor from deviations of indexed reflections.



Plastic strain example (Ni 15% plastic strain).

- Can analyse streak data to determine lattice rotations and predominant active slip systems.



MICROBEAM LAUE

ARTICLE

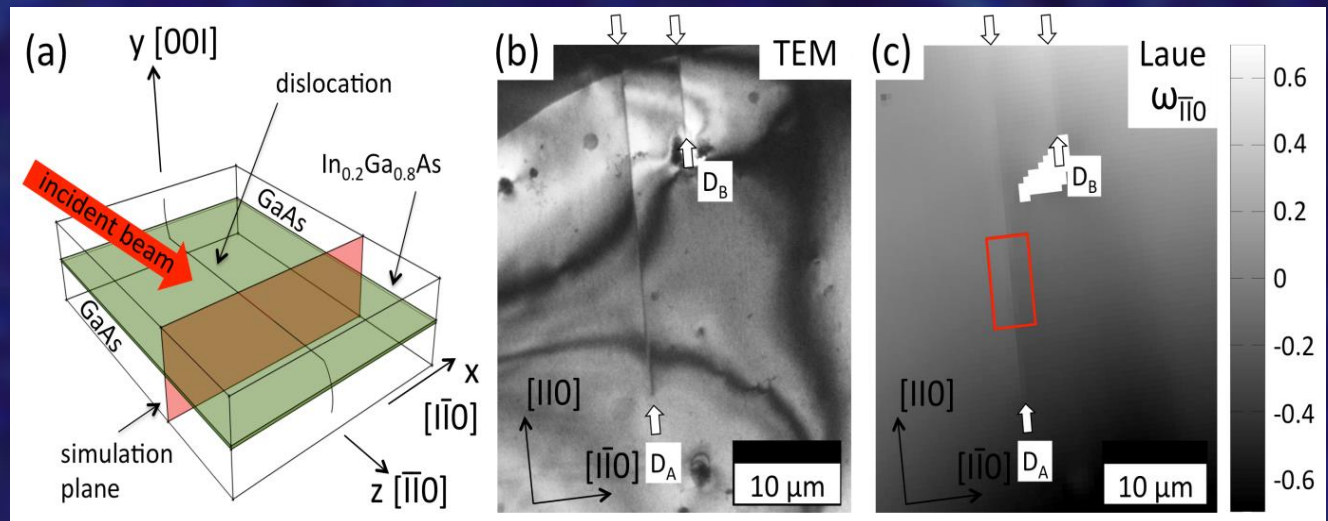
Received 15 Jun 2013 | Accepted 15 Oct 2013 | Published 12 Nov 2013

DOI: 10.1038/ncomms3774

X-ray micro-beam characterization of lattice rotations and distortions due to an individual dislocation

Felix Hofmann¹, Brian Abbey^{2,3}, Wenjun Liu⁴, Ruqing Xu⁴, Brian F. Usher⁵, Eugeniu Balaur^{2,3} & Yuzi Liu⁶

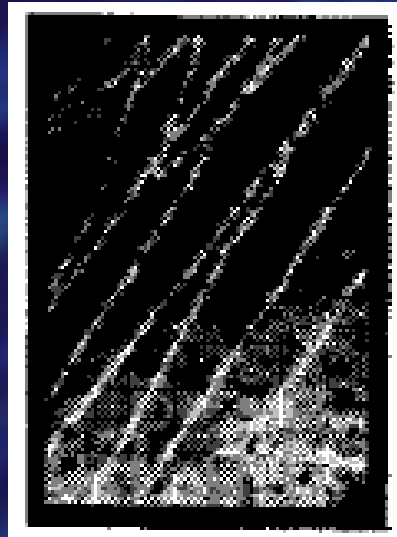
First Laue measurement of a **single dislocation**:
Hofmann & Abbey et al., Nature Comm. 2013





MICROBEAM LAUE

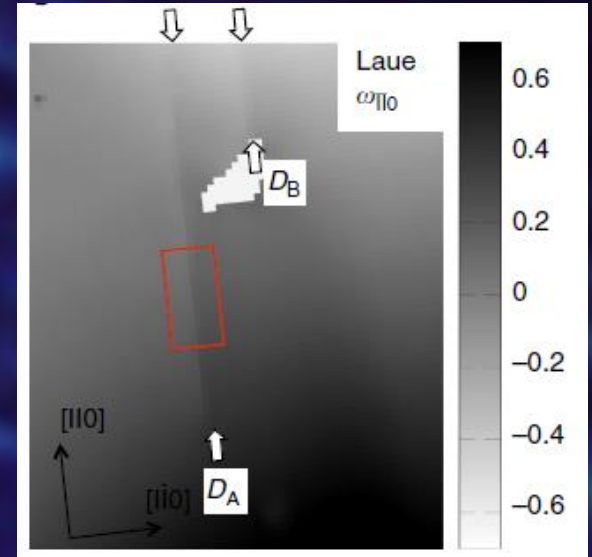
1957



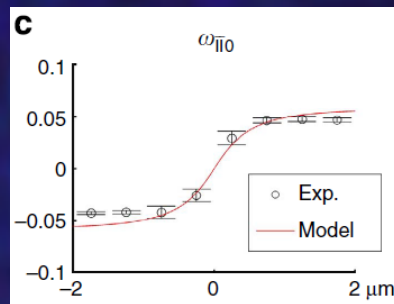
56 years



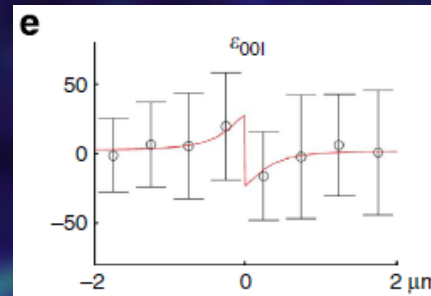
2013



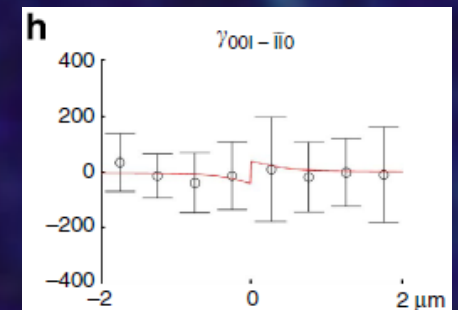
Rotations



Elastic strain



Shear strain

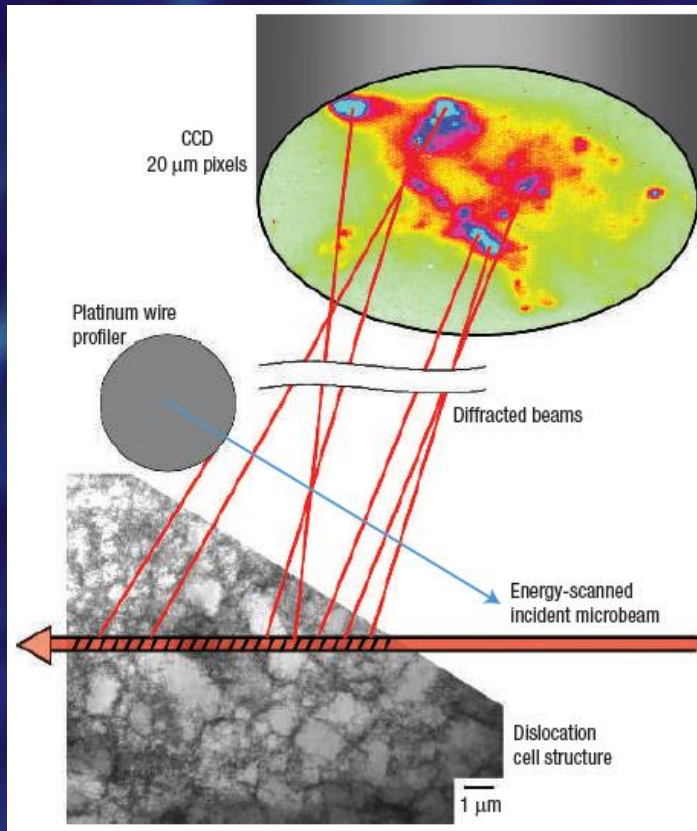


LAUE: SUMMARY



X-ray microbeam measurements of individual dislocation cell elastic strains in deformed single-crystal copper

LYLE E. LEVINE^{1*}, BENNETT C. LARSON², WENGE YANG³, MICHAEL E. KASSNER⁴, JONATHAN Z. TISCHLER², MICHAEL A. DELOS-REYES⁴, RICHARD J. FIELDS¹ AND WENJUN LIU⁵



Can detect groups and individual dislocations inside grains.

However, spatial resolution is determined by spot size, currently $\sim 0.5 \mu\text{m}$. (N.B. ~ 4 -5 times better than XRT).

Can we image samples with nanometer spatial resolutions and on femtosecond timescales?

pm

nm

μm

cm

SHORT COMMUNICATIONS

843

contraction of 2% is largely in a direction normal to the shearing movement:

Parameter of γ : $a = 3.585 \text{ \AA}$;
whence $\frac{1}{2}a\sqrt{2} = 2.535 \text{ \AA}$, $\frac{3}{2}a\sqrt{3} = 4.140 \text{ \AA}$.
Parameters of ϵ : $a = 2.528 \text{ \AA}$, $c = 4.080 \text{ \AA}$.

The mechanism is of the type which produces a 'Widmanstätten' pattern of strain bands; and the contraction associated with the transformation limits the growth of ϵ around each nucleus. A photomicrograph (Fig. 2) confirms both the strain pattern and the absence of massive precipitate, although individual phases cannot be distinguished.

Acta Cryst. (1952). 5, 843

Some implications of a theorem due to Shannon. By D. SAYRE, *Johnson Foundation for Medical Physics, University of Pennsylvania, Philadelphia 4, Pennsylvania, U.S.A.*

(Received 3 July 1952)

Shannon (1949), in the field of communication theory, has given the following theorem: If a function $d(x)$ is known to vanish outside the points $x = \pm a/2$, then its Fourier transform $F(X)$ is completely specified by the values which it assumes at the points $X = 0, \pm 1/a, \pm 2/a, \dots$. In fact, the continuous $F(X)$ may be filled in merely by laying down the function $\sin \pi a X / \pi a X$ at each of the above points, with weight equal to the value of $F(X)$ at that point, and adding.

Now the electron-density function $d(x)$ describing a single unit cell of a crystal vanishes outside the points $x = \pm a/2$, where a is the length of the cell. The reciprocal-lattice points are at $X = 0, \pm 1/a, \pm 2/a, \dots$, and hence the experimentally observable values of $F(X)$ would suffice, by the theorem, to determine $F(X)$ everywhere, if the phases were known. (In principle, the necessary points extend indefinitely in reciprocal space, but by using, say, Gaussian atoms both $d(x)$ and $F(X)$ can be effectively confined to the unit cell and the observable region, respectively.)

For centrosymmetrical structures, to be able to fill in the $|F|^2$ function would suffice to yield the structure, for sign changes could occur only at the points where $|F|^2$ vanishes. The structure corresponding to the $|F|^2$ function is the Patterson of a single unit cell. This has

Acta Cryst. (1952). 5, 843

Unit-cell dimensions and space groups of synthetic peptides. I. Glycyl-L-tyrosine, glycyl-L-tyrosine hydrochloride, glycyl-DL-serine and glycyl-DL-leucine. By T. C. TRANTER, *Wool Industries Research Association, 'Torriton', Headingley, Leeds 6, England*

(Received 5 June 1952)

The data presented here form part of an extended survey of crystalline peptides recently begun by the Wool Industries Research Association. The objects of the investigation are first to obtain some knowledge of the factors influencing the crystallization of these materials; secondly, from their unit-cell dimensions to obtain information regarding the types of molecular arrangements present, and thirdly to select materials suitable for a more detailed X-ray examination.

References

- BARRETT, C. S., GEISLER, H. & MEHL, R. F. (1941). *Trans. Amer. Inst. Min. (Metall.) Engrs.* **100**, 228.
BARRETT, C. S., GEISLER, A. H. & MEHL, R. F. (1943). *Trans. Amer. Inst. Min. (Metall.) Engrs.* **152**, 201.
JONES, F. W. & PUMPHREY, W. I. (1949). *J. Iron Steel Inst.* **163**, 121.
NISHIYAMA, Z. (1936). *Kinzoku no Kenkyu*, **13**, 300.
PARR, J. G. (1952). *J. Iron Steel Inst.* **171**, 137.
SCHEMIDT, W. (1929-30). *Arch. Eisenhüttenw.* **3**, 292.
TROIANO, A. R. & MCGUIRE, F. T. (1943). *Trans. Amer. Soc. Met.* **31**, 340.

twice the width of the unit cell, and hence to fill in the $|F|^2$ function would require knowledge of $|F|^2$ at the half-integral, as well as the integral h 's. This is equivalent to a statement made by Gay (1951).

I think the conclusions which may be stated at this point are:

1. Direct structure determination, for centrosymmetric structures, could be accomplished as well by finding the sizes of the $|F|^2$ at half-integral h as by the usual procedure of finding the signs of the F 's at integral h .
2. In work like that of Boyes-Watson, Davidson & Perutz (1947) on haemoglobin, where $|F|^2$ was observed at non-integral h , it would suffice to have only the values at half-integral h .

The extension to three dimensions is obvious.

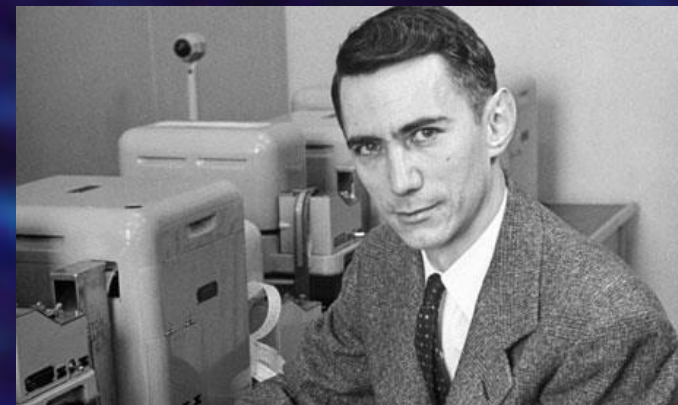
References

- BOYES-WATSON, J., DAVIDSON, E. & PERUTZ, M. F. (1947). *Proc. Roy. Soc. A*, **191**, 83.
GAY, R. (1951). Paper presented at the Second International Congress of Crystallography, Stockholm.
SHANNON, C. E. (1949). *Proc. Inst. Radio Engrs., N.Y.* **37**, 10.

Source of peptides.

Glycyl-L-tyrosine was obtained from Roche Products, Welwyn Garden City, England, and the monohydrochloride was prepared from it by treatment with excess of 2N. HCl, followed by evaporation at room temperature. (Found 12.1% Cl; calculated 12.9%.)

Glycyl-DL-leucine and glycyl-DL-serine were synthesized by the chloroacetyl chloride method first described by



Claude Shannon (1916 – 2001)

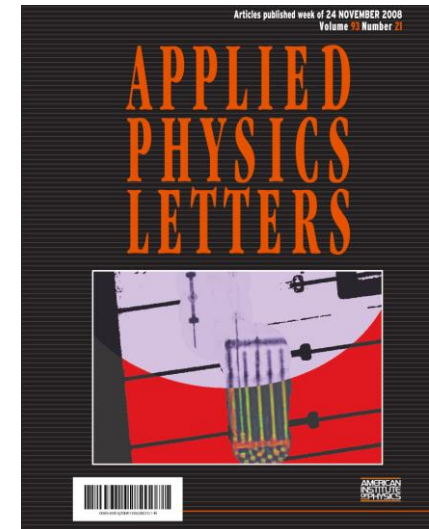
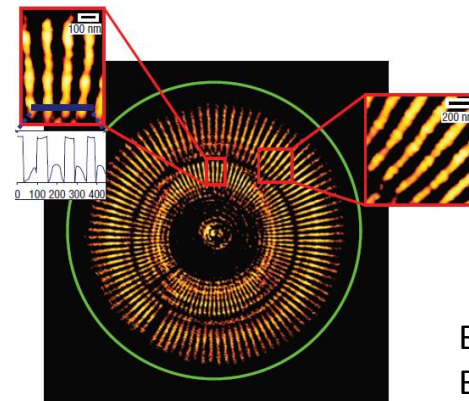
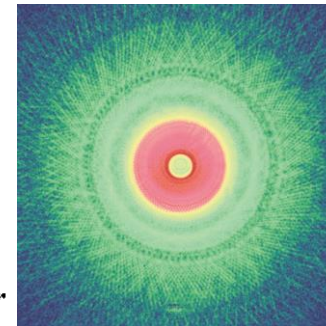
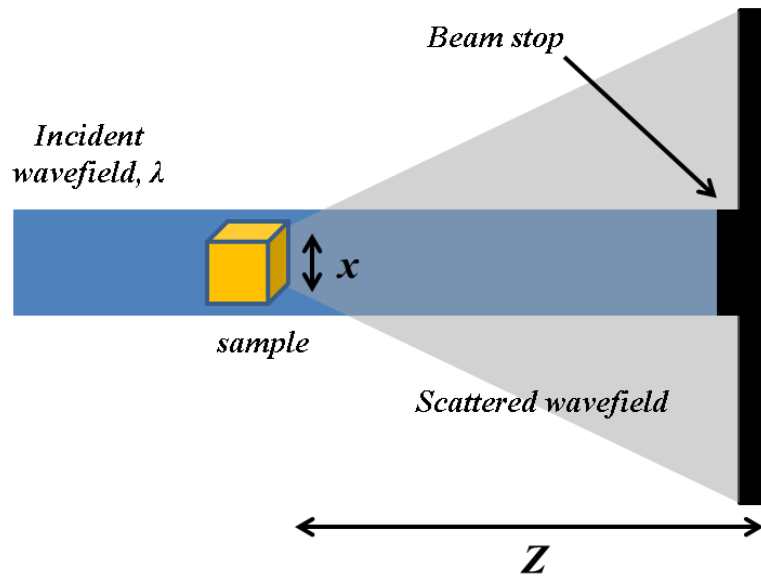


David Sayre (1924 – 2012)

Coherent diffractive imaging is a method for recovering the phase of coherently diffracted intensity.

With the recovered phase one may (with a suitable propagator) recover the complex wavefield exiting the diffracting sample in any plane.

CDI occurs when:
the sample $<$ coherence volume

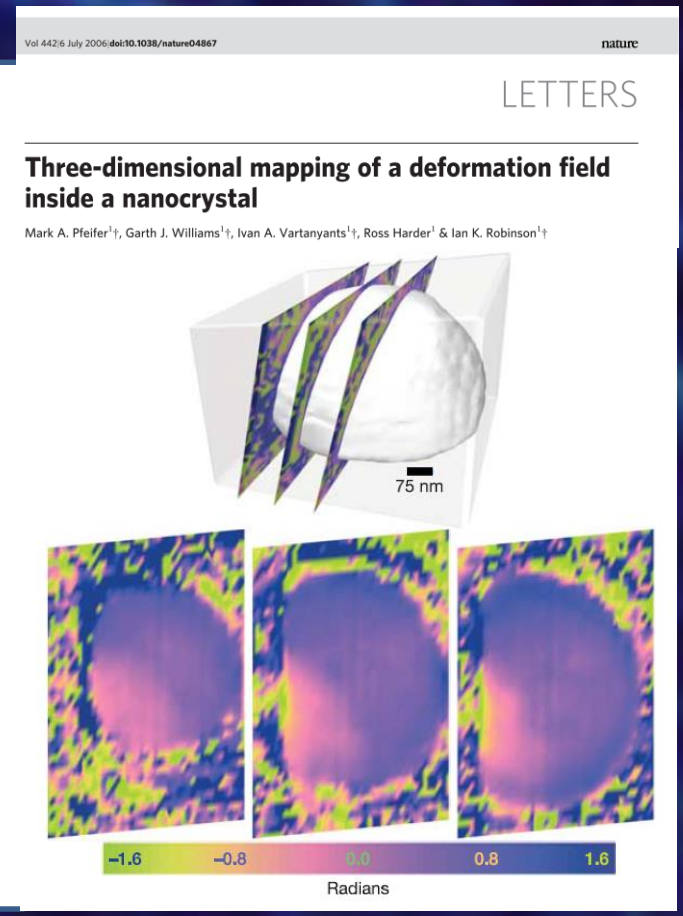
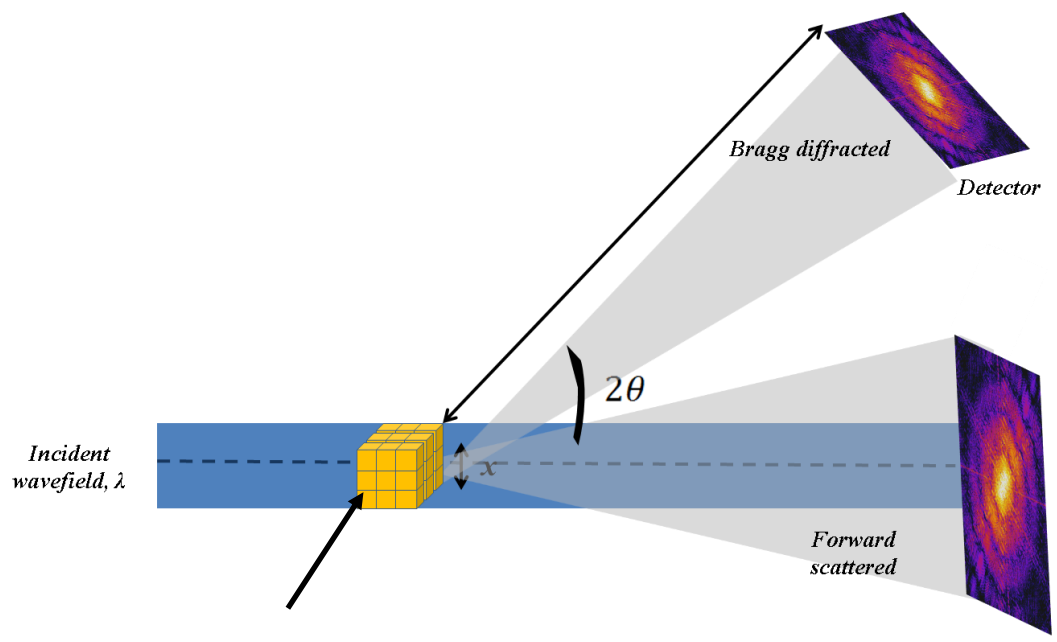


B. Abbey, Nature Phys, 2008
B. Abbey, APL., 2008

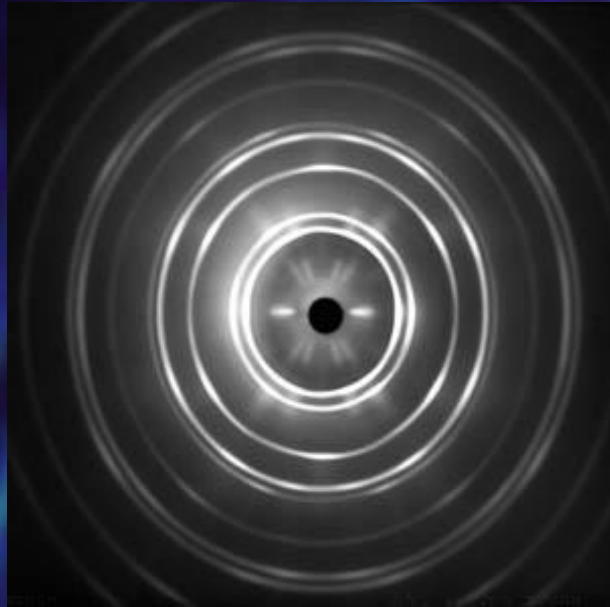


BRAGG COHERENT DIFFRACTIVE IMAGING (BCDI)

2006 – Ian Robinsons group apply coherent imaging to a crystal in Bragg diffraction

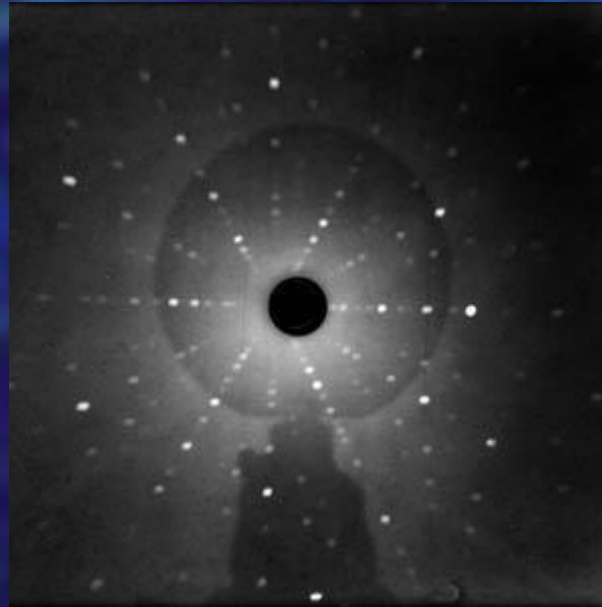


We see lots of this:



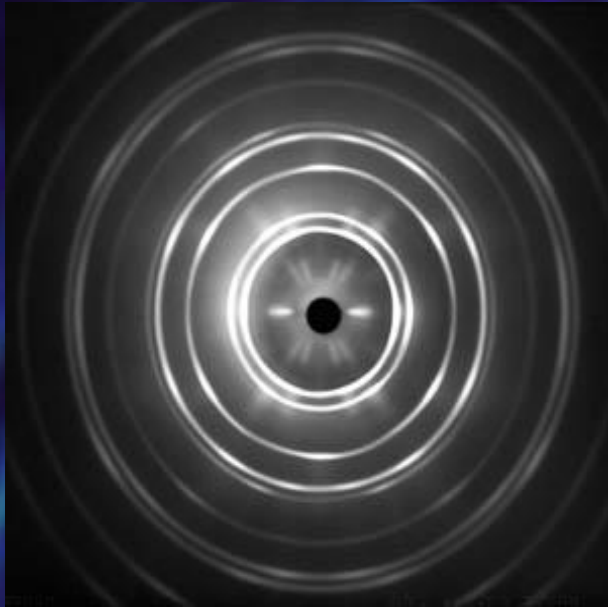
XRPD Al wire

Or this:



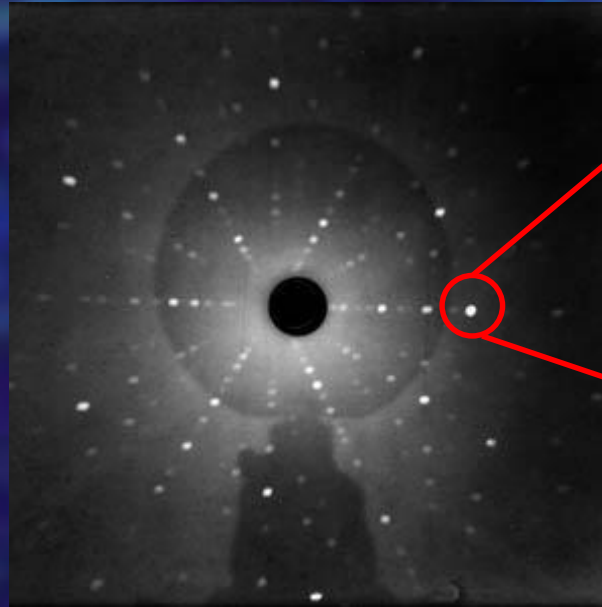
Si crystal

We see lots of this:



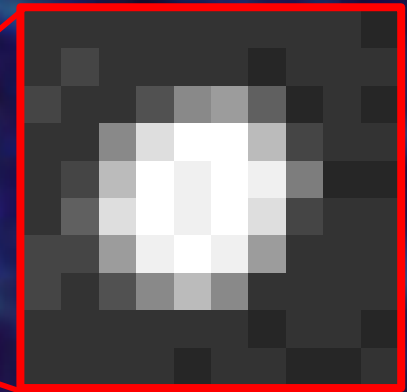
XRPD Al wire

Or this:



Si crystal

I am interested in this:



KEY CONSIDERATIONS

Sample Pixel Width

Propagation Distance

$$\Delta x_s = \frac{\lambda z_{SD}}{N \Delta x_d}$$

Detector Pixel Width

**Detector width determines
your highest resolution**

~5-20 nm

$$q \approx \frac{\rho_d}{\lambda z_{SD}}$$

Detector coordinate

Reciprocal Space
Vector (1/d)

**Detector pixel size
determines the maximum
imaging area**

~ < 2 μm

Large Rotations: ← XRT, Laue, XRD, etc.

- Neglect fine scale structure of reflection.
- Consider change in position, i.e. large rotations of whole reflection.
- Evaluate quantities like overall FWHM of the whole reflection.

Small Scale rotations:

- Consider structure of each reflection.
- No large rotations, i.e. offsets in the reflection position.

Large Rotations:

- Neglect fine scale structure of reflection.
- Consider change in position, i.e. large rotations of whole reflection.
- Evaluate quantities like overall FWHM of the whole reflection.

Small Scale rotations:

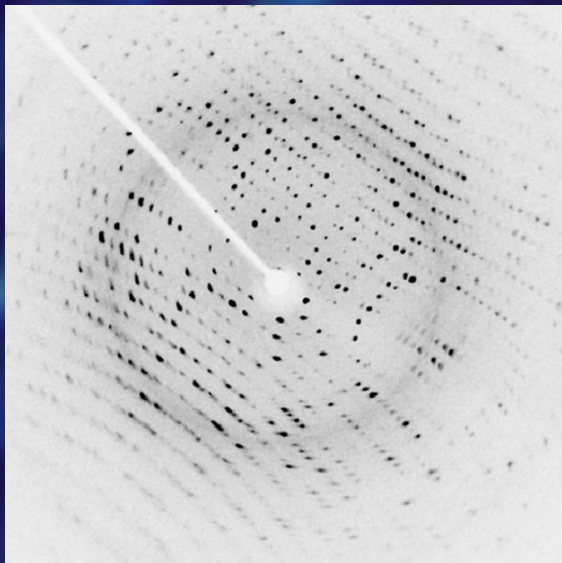


Coherent X-ray Diffraction

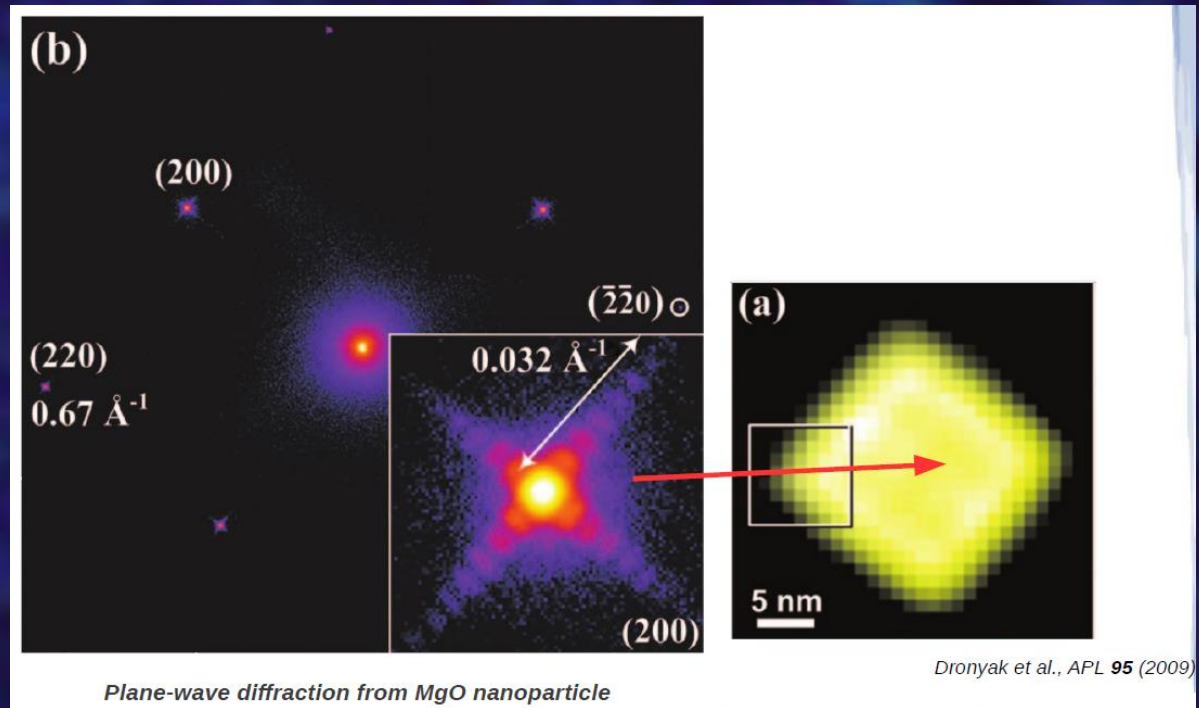
- Consider structure of each reflection.
- No large rotations, i.e. offsets in the reflection position.

BRAGG COHERENT DIFFRACTIVE IMAGING (BCDI)

Incoherent large crystal



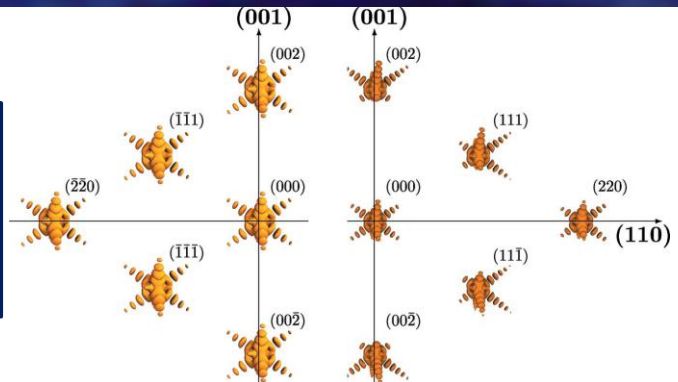
Coherent small crystal/grain/beam



BRAGG COHERENT DIFFRACTIVE IMAGING (BCDI)

Bragg peaks for a perfect crystal:

- a. are centrosymmetric,
- b. the maximum is at the centre and,
- c. are all identical for each h_n .



Bragg peaks for strained crystal:

- a. are noncentrosymmetric and,
- b. are all different for each h_n .

Crystal electron density

Displacements

$$I(\mathbf{q}) \propto \left| \int_0^\infty \rho_L(\mathbf{r}) s(\mathbf{r}) e^{i\mathbf{q} \cdot \mathbf{r}} e^{i\mathbf{q} \cdot \mathbf{u}(\mathbf{r})} d\mathbf{r} \right|^2$$

Bragg Intensity

Shape function

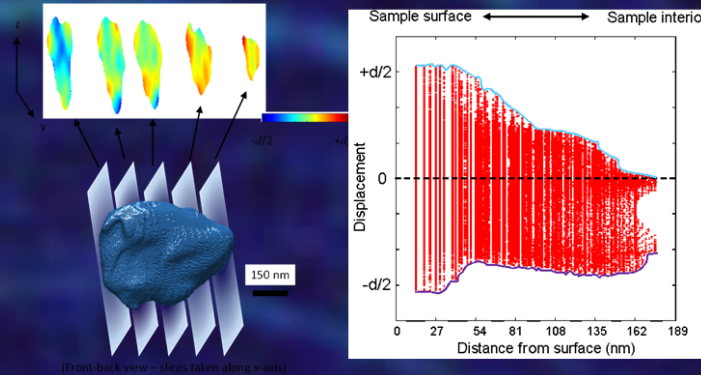
Any asymmetries are indicative of strain.

BRAGG COHERENT DIFFRACTIVE IMAGING (BCDI)

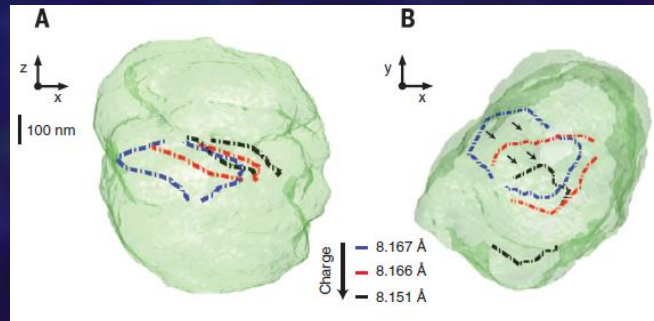
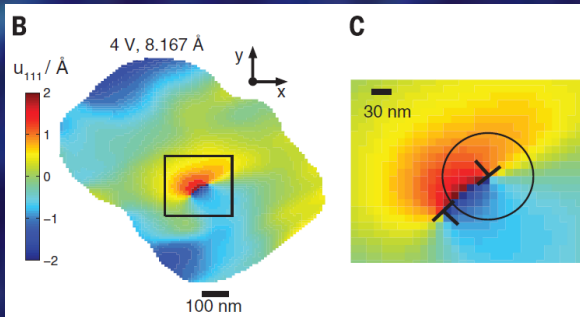
What can be done so far? Some examples:

Characterising disorder in nanodiamonds:

Maqbool et al. *J. Nanotech*, 2016 (in press) (LTU)



High-resolution characterisation of single defects in nanocrystals:



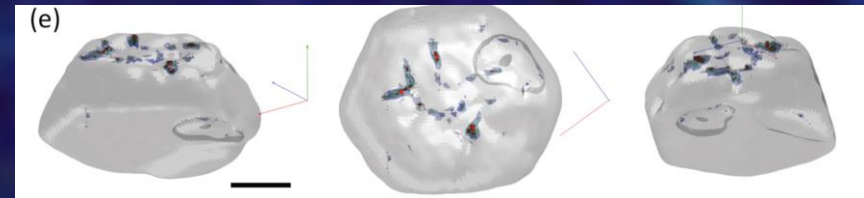
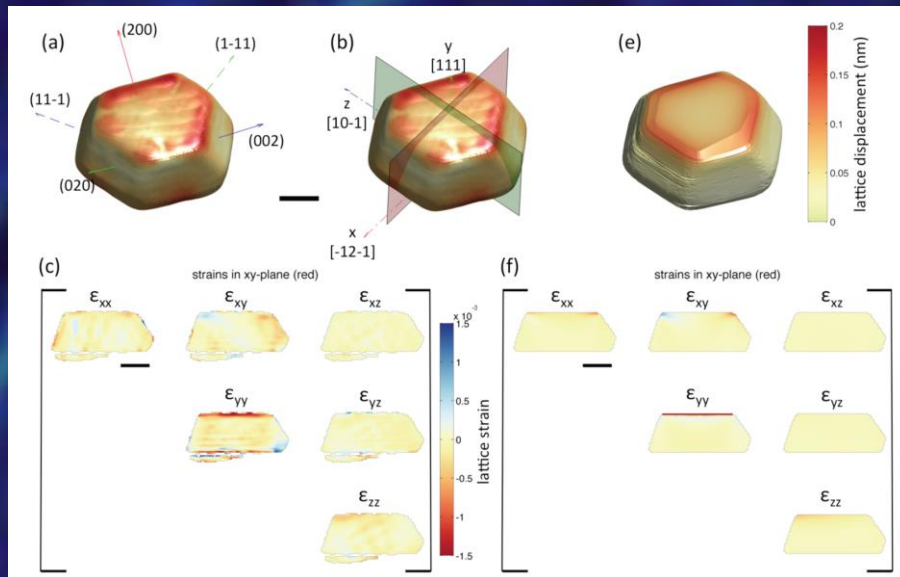
Ulvestad et al. *Science*, 2015 (UCSD)

Measurements on single buried grains also possible.

BRAGG COHERENT DIFFRACTIVE IMAGING (BCDI)

Have looked at disorder, what about recovery of strain tensor?

High-resolution strain mapping in ion implanted nanocrystals using 5 reflections:



iso-surfaces of von Mises stress, corresponding to 300 MPa (blue), 400 MPa (green) and 500 MPa (red). Three different viewpoints are shown. Scale bars are 300 nm in length in

F. Hofmann et al., PNAS (submitted), 2016

Full lattice strain tensor in Au nanocrystal after Ga ion implantation.

Coherent diffraction + protein crystallography

Dilanian et al. Acta cryst A, 2016

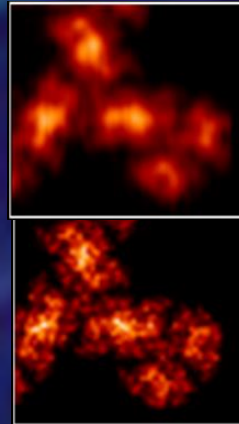
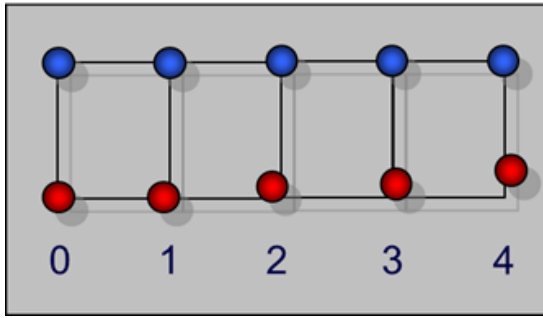
Chapman et al. Nature, 2016

Acta Crystallographica Section A
Foundations of
Crystallography
ISSN 0108-7673

Continuous X-ray diffractive field in protein nanocrystallography

Ruben A. Dilanian,^{a*} Victor A. Streltsov,^b Harry M. Quiney^a and Keith A. Nugent^a

Model of the disorder

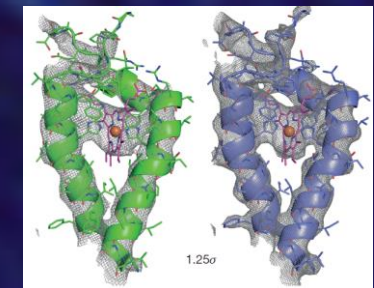
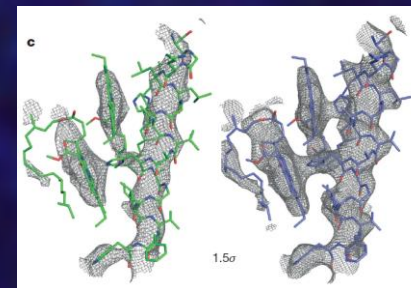
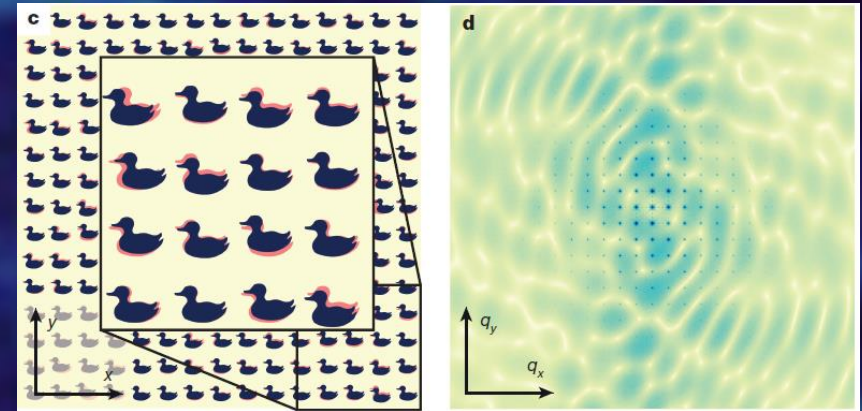


$$I(\mathbf{q}) = |F(\mathbf{q})|^2 \cdot \tilde{\Lambda}(\mathbf{q})$$

$$\tilde{\Lambda}(\mathbf{q}) = \sum_{jk} \exp(i\mathbf{q} \cdot \mathbf{R}_j) g_{jk}(\mathbf{q}) \exp(-i\mathbf{q} \cdot \mathbf{R}_k)$$

where $F(\mathbf{q})$ is the molecular (unit-cell) form-factor, $\tilde{\Lambda}(\mathbf{q})$ is the interference function and the summations are over all unit cells.

The complex factor $g_{jk}(\mathbf{q})$ incorporates information about disorder (perfect order restored if $g_{jk}(\mathbf{q}) = 1$, independent of \mathbf{q}).

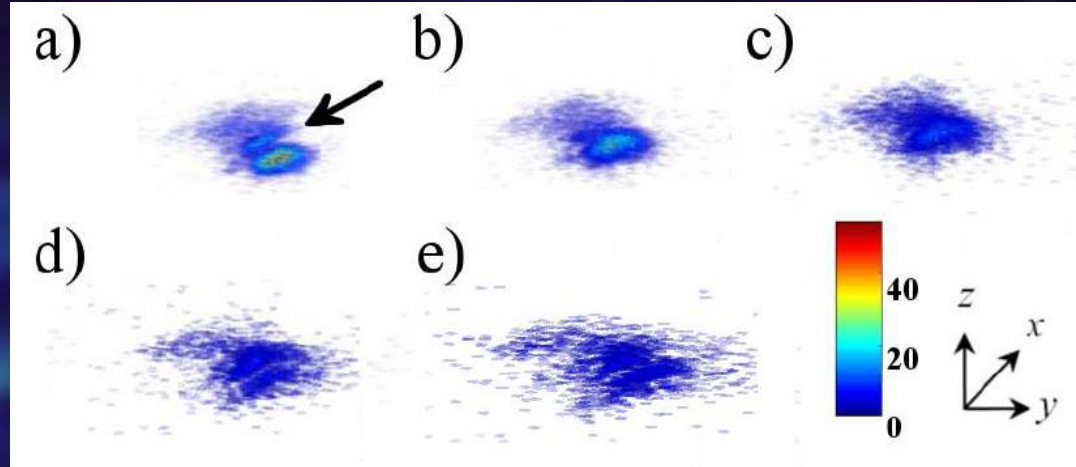


4.5 angstrom

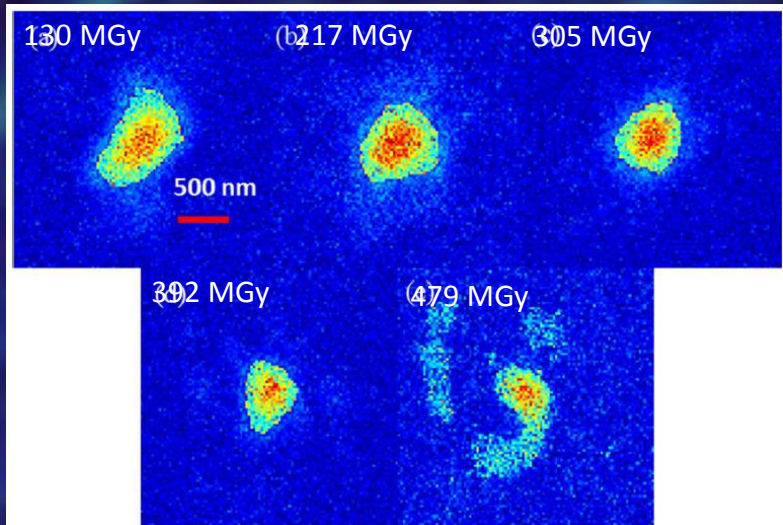
3.5 angstrom



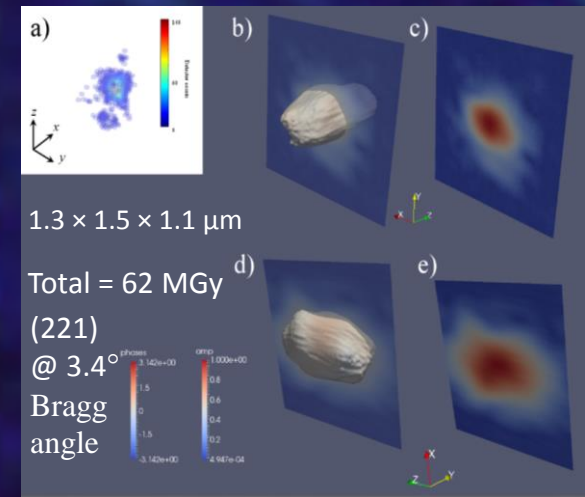
Hannah Coughlan
4th year PhD student



Coughlan et al. Str. Dyn. 2015



Coughlan et al. J. Optics. 2016



For comparison XFEL delivers ~ 700 MGy in < 100 fs.
Dose required for single BCDI image is < 2 Mgy (1-5 s exp.).

PROJECT IDEAS/SUMMARY

- Looking for a good student to continue Hannah's work in super-resolution synchrotron based crystallography

- Many open questions:

e.g. Can we use current crystallography beamlines to make these measurements?

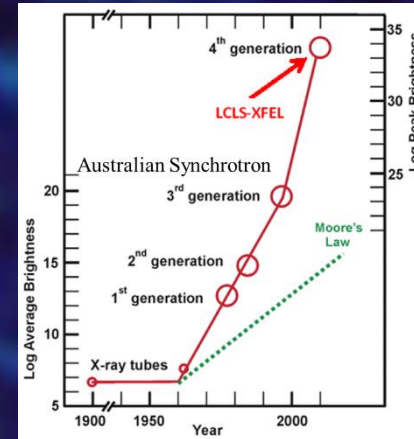
How many reflections need to be oversampled?

Can we model/estimate the potential benefits to microcrystallography?

- We have plenty of data and more results to come, but currently looking for someone to help continue this project.

X-ray Free Electron Lasers

The LCLS in Stanford is the worlds first 'hard' X-ray free electron laser.

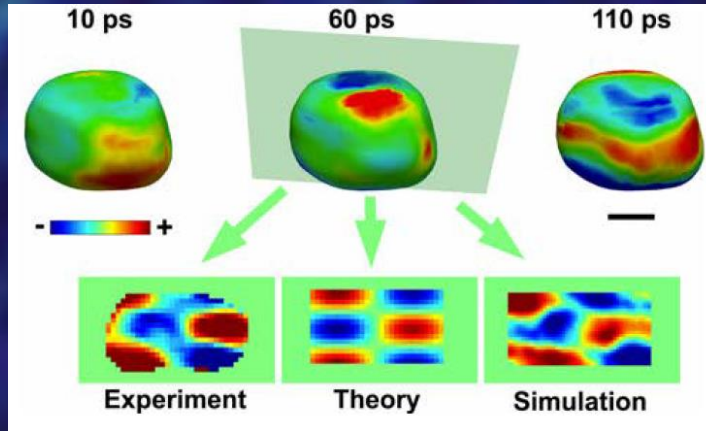
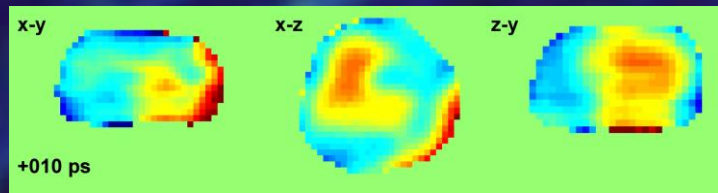
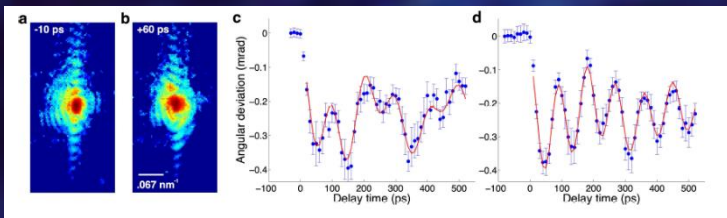


The SLAC accelerator can accelerate electrons up to 50 GeV. It's > 3 km long and the longest linear accelerator in the world. Claims to be "the world's straightest object." [11]

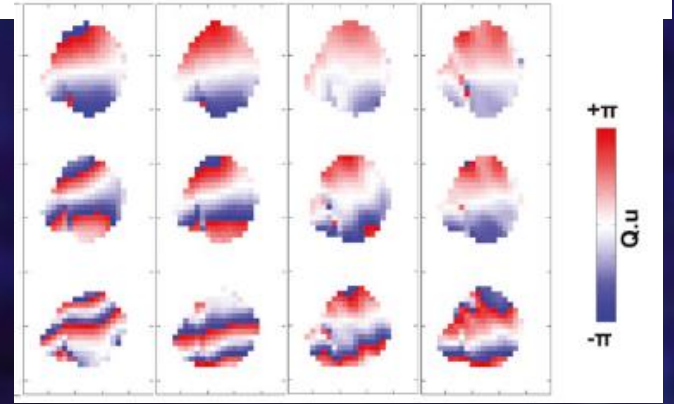
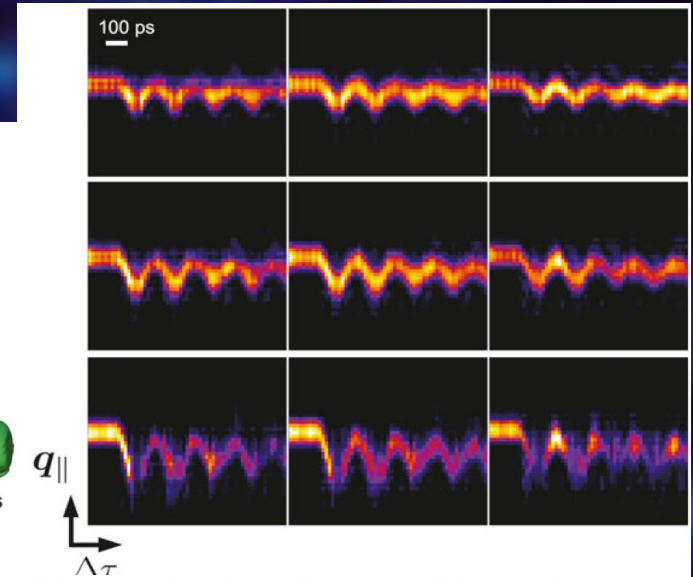
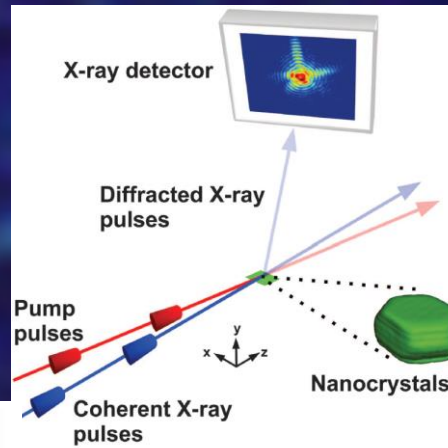
The main accelerator is buried 20 m below ground and the building above the beamline is the longest building in the US. The LCLS is a partial reconstruction of the last ~1/3 of the original accelerator.

STRAIN AT THE NANOSCALE IN 4D USING XFELS

Clark et al, Science, 2013



Clark et al, PNAS, 2015



PROs

Provides spatial resolution well-below the probe size.

Only technique that can image dislocations and defects in 'bulk' materials with nm spatial resolution.

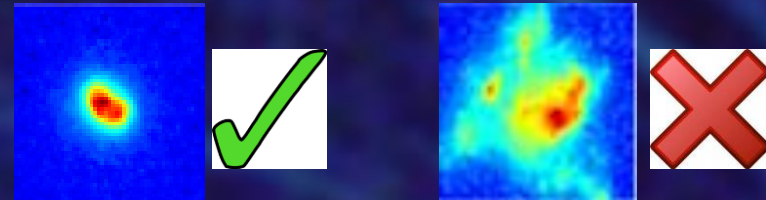
Can image single dislocations and their associated strains down to $\sim 1/10$ lattice spacing sensitivity.

When combined with XFELS can be used for probing dynamics on a femtosecond timescale.



CONs

Needs samples with reasonable crystallinity (fairly low mosaicity)



Extended samples ($>2 \mu\text{m}$) still a work in progress.

Max energy (due to coherence constraints) $\sim 13 \text{ keV}$.

At the moment requires specialist expertise for data analysis.

XFEL induced structural changes

Investigating the dynamical interactions of matter with intense XFEL sources using C_{60} as a model system.

Brian Abbey, Ruben A. Dilanian, Connie Darmanin, Rebecca A. Ryan, Corey T. Putkunz, Andrew V. Martin, David Wood, Victor Streltsov, Michael W. M. Jones, Naylyn Gaffney, Felix Hofmann, Garth J. Williams, Sébastien Boutet, Marc Messerschmidt, M. Marvin Seibert, Sophie Williams, Evan Curwood, Eugeniu Balaur, Andrew G. Peele, Keith A. Nugent and Harry M. Quiney

First Australian team wins beam time on world's most powerful X-ray laser.

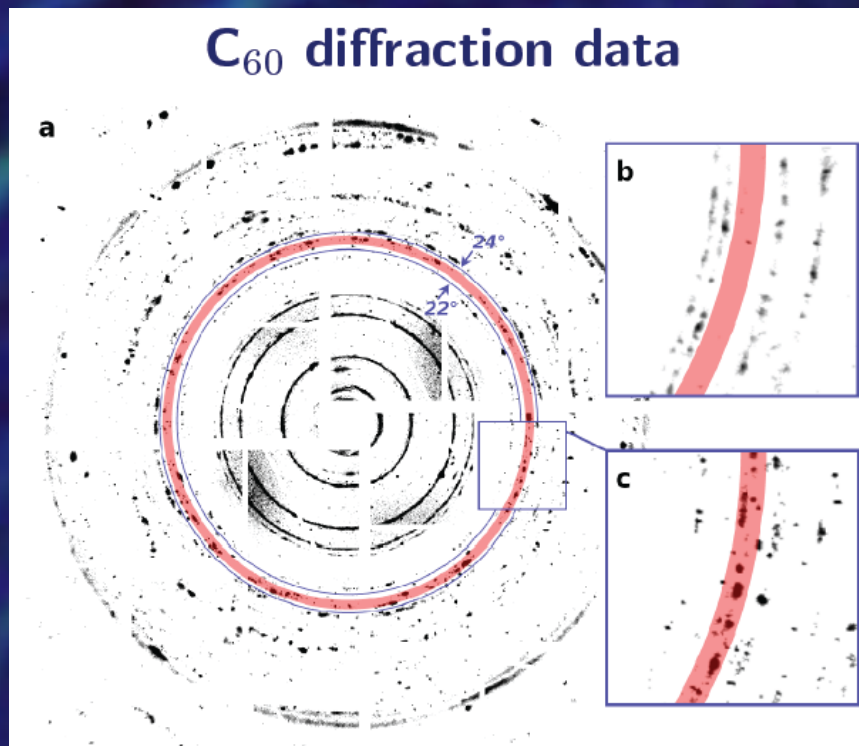


[NewsRx Health & Science](#)

June 26, 2011 | [Copyright](#)

Australian researchers investigating the structure of membrane proteins for improving drug development are the first Australians to be awarded access to the world's most powerful X-ray laser.

XFEL induced structural changes

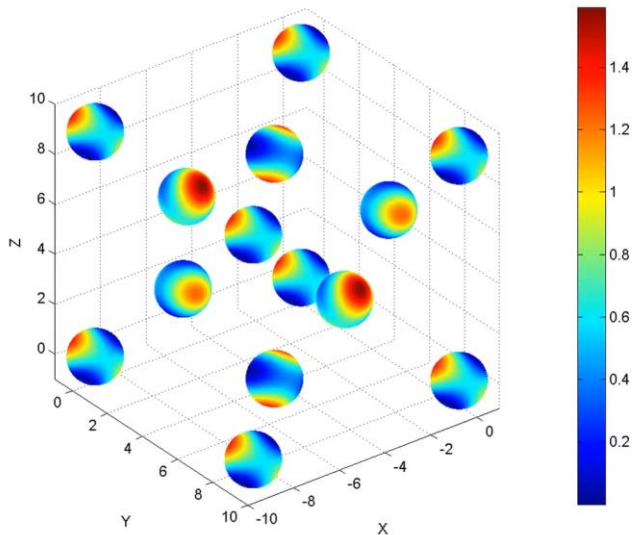


What we observed was a **wholesale modification** of the C₆₀ structure factors dependant only on the incident intensity.

Such a structure/diffraction pattern has never been observed for C₆₀ before.

Could have implications for future XFEL nanocrystallography.

XFEL induced structural changes



First 2 fs of rearrangement of C60
FCC unit cell. (HMO, modelled as an
'open quantum system')

Look into crystal ball

Melbourne scientists in molecule breakthrough

MARK DUNN

MELBOURNE researchers have accidentally discovered how to transform molecules into a new type of crystal — a potential breakthrough for next-generation drug developments — using the world's most powerful X-ray emitting light 10 billion times brighter than the sun.

The work, led by Associate Professor Brian Abbey at La Trobe University, has overturned more than a century of accepted thinking in crystallography, the science of determining arrangement of atoms in solids.

"Currently, crystallography is the tool used by biologists and immunologists to probe the inner workings of proteins

and molecules, the machines of life," Prof Abbey said.

"Being able to see these structures in new ways will help us to understand interactions in the human body and may open new avenues for drug development."

The research is being done in collaboration with Associate Professor Harry Quiney at the University of Melbourne.

An international team of more than 20 scientists used the world's first hard X-ray free electron laser (XFEL), based at Stanford University in the US, on Buckminsterfullerene crystals, or "Buckyballs", and found they altered shape from one like a soccer ball panel to an oval pattern.

"It was like smashing a wal-

nut with a sledgehammer and instead of destroying it and shattering it into a million pieces, we instead created a different shape — an almond," Prof Abbey said.

Because other X-ray sources deliver their energy much slower than the XFEL, all previous observations found they randomly melted or destroyed the crystal.

"We were stunned. This is the first time in the world that X-ray light has effectively created a new type of crystal phase," said Assoc Prof Quiney, head of the Melbourne Theoretical Condensed Matter Group.

mark.dunn@news.com.au

Herald Sun, Sep, 2016

Abbey et al., Science Adv. 2016

Thank you for your attention!

Materials characterisation and XFEL science group:

See: <http://www.latrobe.edu.au/physics/research/x-ray-science/materials-characterisation>